Study of N-linked Glycosylation of Mouse Peripheral Myelin

A MALDI-TOF mass spectrometry approach

Matteo Gaglianone

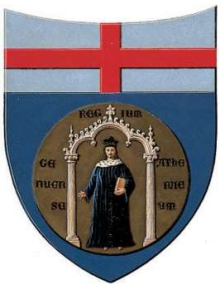

PhD in Experimental Medicine

Curriculum Biochemistry

XXX cycle

University of Genova

2017

Supervisor: Michela Tonetti BIO/10

Index

Abbreviations

Peripheral Nervous System (PNS)

Central Nervous System (CNS)

Schmidt-Lanterman incisure (SLIs)

Myelin Protein Zero (MPZ or MP0)

Myelin Proteolipid (PLP)

Myelin-associated glycoprotein (MAG)

Myelin Basic Protein (MBP)

Myelin Associated Glycoprotein (MAG)

Peripheral Myelin Protein (PMP22)

Fatty Acid Binding Proteins (FABP)

Charcot-Marie-Tooth type 1B (CMT1B)

Charcot-Marie-Tooth (CMT)

Congenital Disorders of Glycosylation (CDG)

Phosphomutase-2 (PMM2)

Diethylaminoethanol–High Performance Liquid Chromatography (DEAE-HPLC)

Human Natural Killer-1 (HNK-1)

Matrix-Assisted Laser Desorption/Ionization Time-of-flight Mass Spectrometry (MALDI-TOF)

Mass Spectrometry (MS)

Mass/Charge ratio (m/z)

Liquid Chromatography–Mass Spectrometry (LC-MS)

Protease Inhibitor Cocktails (PIC)

Ammonium Hydrogen Carbonate (AMBIC)

3,4-diamino-benzophenone (DABP)

Introduction

1.1 Myelin

The myelin sheath is a greatly extended and modified plasma membrane wrapped around the nerve axon in a spiral fashion. Myelin facilitates saltatory transmission of electrical impulses along axons (Raine CS 1984).

The most important function of myelin is to increase the conduction velocity of the axon without increasing axon diameter. Myelin works like an electrical insulator, allowing the nerve impulses to jump between unmyelinated regions of the axon. These regions, called nodes of Ranvier, are located between the myelinated area and have very similar structure in CNS (Central Nervous System) and PNS (Peripheral Nervous System). In myelinated axon, the node of Ranvier is the location of sodium channel.

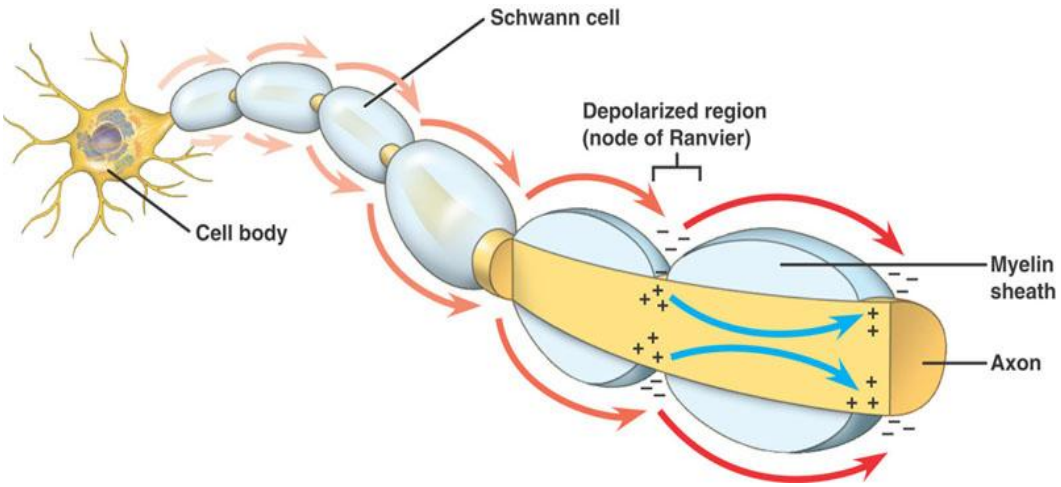

Figure 1. General representation of myelin saltatory impulse.

The myelin sheath has two distinct regions, compact myelin and non-compact myelin. Non-compact myelin contains cytoplasm and is thought to

be involved in cell signaling, transport and the physiological homeostasis of myelin. Non-compact myelin is composed by Schmidt-Lanterman incisures (SLI), paranodal loops and outer mesaxons.

SLIs are small pockets containing residual cytoplasm, which are formed during the myelination process. These clefts provide communication channels between layers by connecting the Schwann cell and the deepest layer of the myelin sheath (Small J et al. 1987).

The paranodal loops flank the nodes of Ranvier and are rich in cellular junctions that provide a barrier between the extracellular space and the periaxonal space (Spiegel I et al. 2002). In the PNS the myelin membranes originate from the Schwann cells, while in the CNS they are formed by oligodendrocytes.

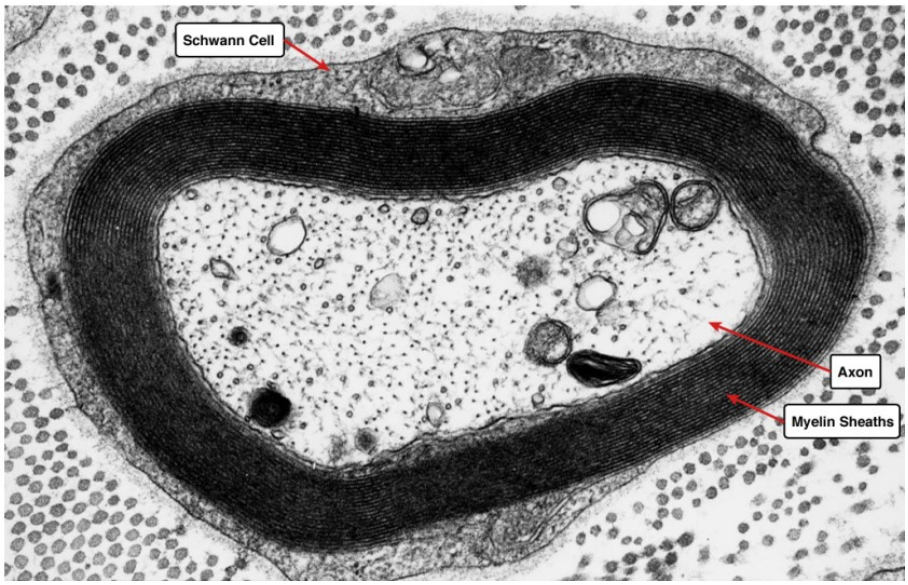

Figure 2. Myelinated Axon EM. This electron microscopy image shows a cross section of a myelinated nerve in the peripheral nervous system. The Schwann cell wraps around the axon to envelop it in a myelin sheath that functions as an electrical insulator. (http://medcell.med.yale.edu/histology)

Schwann cells derive from the neural crest. During development, they undergo several differentiation steps, from the immature stage to the non-myelinating, promyelinating and actively myelinating cells. Moreover, after nerve injury, myelinating cells can convert to a highly specialized cell (the repair Schwann cell) that is essential for nerve regeneration (Arthur-Farraj PJ et al. 2012).

Characteristic gene expression changes accompany each stage of Schwann cell development and various transcription factors are up- and down-regulated to coordinate their maturation from neural crest cells to mature myelinating or non-myelinating cells. The genes mainly involved in the differentiation of the Schwann cells are *sox10*, *krox20* (Egr2) and *oct6*. *Sox10* is the first gene activated during the detachment from the neural crest and stay up-regulated in migrating cells and immature cells (Scherer SS et al. 2008). *Oct6* is activated in promyelinating cells and together with *sox10* and *krox20* support the final differentiation in Schwann cells. *Sox10* and *krox20* regulation will be also necessary for the maintaining of Schwann cell functions and properties (Scherer SS et al. 2008).

The most important protein up-regulated during this promyelinating pathway is Myelin Protein Zero (MPZ). Consequently, MPZ is also the most abundant proteins in compact PNS myelin (Quarles RH et al. 2006).

The importance of proper PNS myelin function is highlighted by the devastating effects of demyelination in several diseases, such as acquired neuropathies or in genetic syndromes (Scherer SS et al. 2008).

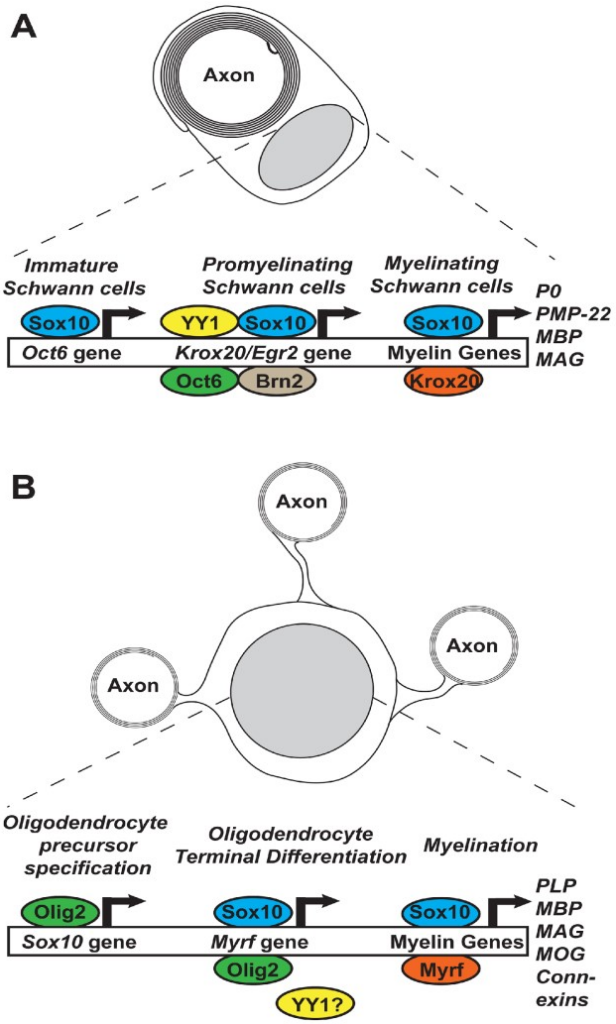

Figure 3. Main genes involved in the differentiation of the Schwann cells and the oligodendrocytes. (Emery B et al. 2013)

1.1.1 Myelin composition

Myelin is composed of roughly 70% lipid and 30% proteins; while lipid composition is similar, there are important differences between CNS and PNS myelin proteins. While some are found in both systems, such as Myelin Associated Glycoprotein (MAG) and Myelin Basic Protein (MBP), others are more specific for PNS myelin, as Myelin Protein Zero (MPZ or P0) and Peripheral Myelin Protein (PMP22) (Quarles RH et al. 2006).

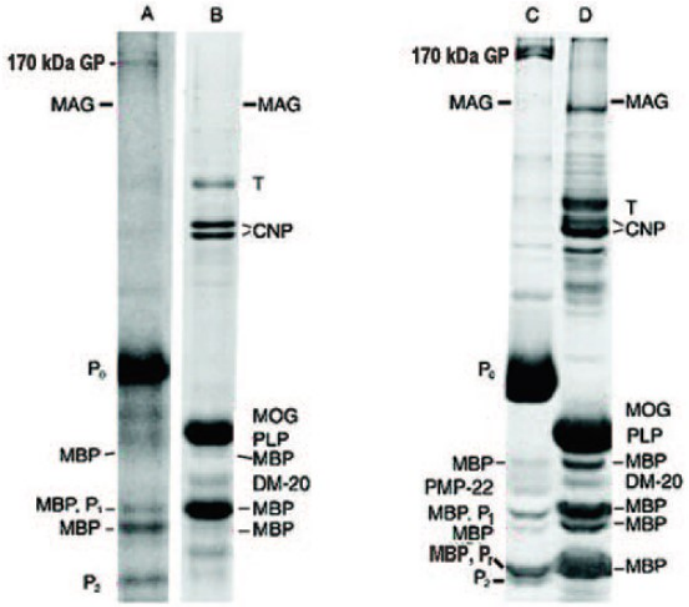

Figure 4. SDS-Polyacrilamide gel electrophoresis of myelin proteins. A) Human PNS myelin, B) Human CNS myelin C) Rat PNS myelin D) Rat CNS myelin. There is a high similarity in the PNS, where only MPZ is expressed at high level. (Quarles RH et al. 2006)

The MBPs are proteins localized at the plasma membrane; evidences suggest a homodimer structure that may have an important role in stabilizing myelin. The MBP genes can undergo alternative splicing and, as a result, there are different isoforms, which the most abundant is the 18.5 kDa form (Quarles RH et al. 2006).

PMP-22 is a glycoprotein with four hydrophobic transmembrane domains: it is found in the compact myelin and it characterised by a single N-glycosylation site. It is less abundant than MPZ and is not nerve specific because it can be found in many other tissues. It is present in a small amount in the plasma membranes of both myelinating and nonmyelinating Schwann cells, suggesting a role in maintenance and assemblage of myelin structure (Quarles RH et al. 2006).

MAG is situated in the periaxonal membrane of myelin and in the Schwann cell membranes of the Schmidt-Lanterman incisures. MAG control adhesion and signalling between myelinating cells and axons and maintains a defined spacing between the innermost myelin surface and the axon surface (Pronker MF et al. 2016).

P2 protein is a positively 15 kDa charged protein, member of cytoplasmic Fatty Acid Binding Proteins (FABP). Larger amounts of P2 protein are found in the compact myelin (Kirschner DA et al. 1992), but there is no experimental evidence of its function and role. P2 have a high homology with the proteins that interact with membrane lipid suggesting its involvement in the assemblage of the myelin sheath (Quarles RH et al. 2006).

1.1.2 MPZ

The major difference on the protein composition between CNS and PNS is that MPZ replace almost completely PLP as the most abundant protein. These proteins may have a similar role in the formation and homeostasis of myelin, but sequence and post-translational modifications are very different.

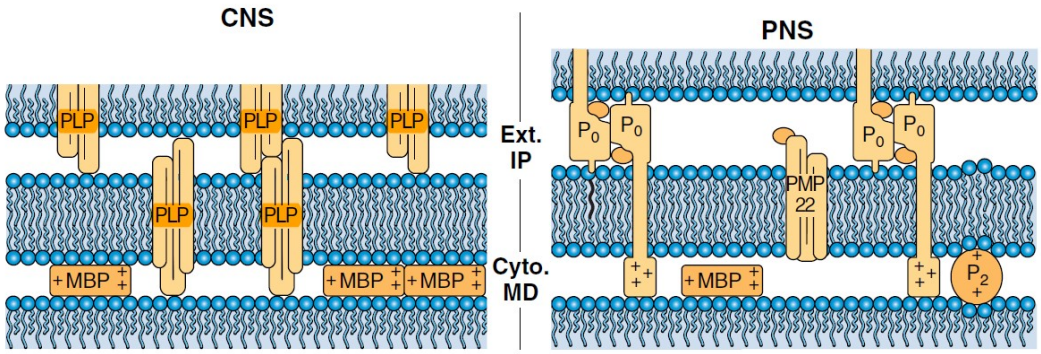

Figure 5. MPZ (P_0) and PLP. Copyright © 2012, American Society for Neurochemistry

Previous studies indicated that MPZ is the major component of PNS myelin, accounting for more than 60% of total proteins (Eichberg J 2002). However, a recent proteomic analysis of PNS myelin re-evaluated these estimates, revealing that MPZ represents 21% of total proteins, followed by periaxin (16%) and myelin basic protein (MBP, 8%) (Patzig J et al. 2011).

MPZ is a transmembrane glycoprotein of 25 kD expressed by Schwann cell. MPZ has an extracellular Ig-like domain, which contains a single site for N-glycosylation and the glycans at this site are very heterogeneous. The intracellular domain can undergo through other post-translational modification that includes phosphorylation and acylation (D'Urso et al. 1990; Eichberg & Iyer, 1996).

Evidence seems to suggest that the Ig-like extracellular hydrophobic domain (Figure 6.) ensure the right formation of the multi-lamellar myelin sheath and myelin compaction through homophilic binding (Kirschner, DA 2004).

Figure 6. Crystal structure of the extracellular domain of human MPZ protein https://www.ebi.ac.uk/pdbe/entry/pdb/3oai/citations

The N-glycans attached to the extracellular domains of MPZ could have different roles. Glycans, together with the large Ig-like domains, may be responsible for the wider space between extracellular surfaces in PNS myelin or, as some studies suggest, may have an important role in the interaction among the adjoining MPZ molecules (Shapiro et al. 1996).

Autosomal dominant mutations of MPZ lead to the development of Charcot-Marie-Tooth type 1B (CMT1B) in patients, who develop peripheral neuropathies of different gravity and age of onset, depending on the mutation involved (Scherer SS et al. 2008).

1.2 Myelin Glycosylation

1.2.1 Glycosylation

Glycosylation is a multi-step process (nucleotide sugar biosynthesis and transport, sugar transfer and glycoprotein secretion) that, if altered, may compromise the function of the modified proteins. Proteins with altered glycosylation can have a gain/loss of function and lead to a pathogenic condition.

N-glycosylation is a particular modification in which a glycan is attached to proteins at asparagine residue by an N-glycosidic bond. In eukaryotes, the first sugar bound to the protein is N-acetylglucosamine (GlcNAc). N-glycans have a high diversity and they have important functions, like quality control of protein folding, cell adhesion and protein interactions (Stanley P et al. 2009).

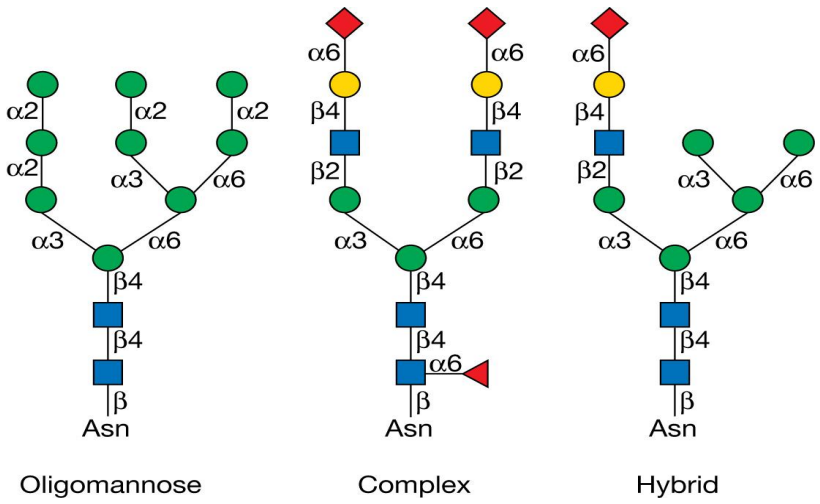

Figure 7. Representation of different type of N-glycans. In this figure can be notice the common N-Glycans core composed by GlcNAc2-Man3. (Essentials of Glycobiology, Chapter 9 fig 1)

N-glycans are added to membrane and secreted proteins at a particular consensus sequence that is Asn-X-Ser/Thr. The importance of this

modification is given by the fact that 70% of proteins have the consensus sequence for N-glycosylation and 70% of these sequences are N-glycosylated. Three types of N-linked structures are present: i) the oligomannose type, which contains only mannose residues beside the chitobiose core; ii) the complex type, in which both antennae are substituted, generally by lactosamine units; and iii) the hybrid type, which presents both type of structures on the two antennae, as shown in Figure 7. The complex types can harbour different numbers of antennae, which generally contain a terminal sialic acid or more complex structure, such as antigens of the Lewis system (Stanley P et al. 2009).

For the study of N-glycans, it is possible to use some enzyme that release the sugar chains. Peptide N-Glycosidase-F (PNGaseF) for example, is a bacterial enzyme that cleaves the N-glycosydic bond, thus releasing the complete glycan. Endoglycosidase H, cleave the O-glycosydic bond between the two core GlcNAc residues (Stanley P et al. 2009).

In O-glycosylation, glycans are attached to a Serine or Threonine residue. This modification is typical of mucin-type glycoproteins, in which the glycan portion is essential for their function. However, this modification can be found in many different glycoproteins and the glycan chains may highly variable. Proteins can attach either a single GalNAc or more than 20 sugar residues, as for instance it occurs for the antigens of the ABO blood group (Stanley P et al. 2009). There is not a particular consensus sequence for O-glycosylation because the first enzymes involved in this pathway (the GalNAc transferases) have more isoforms, which recognise different substrates. In this case, recognition is due to the tridimensional structure of the polypeptide chain.

1.2.2 Congenital Disorders of Glycosylation

The Congenital Disorders of Glycosylation (CDG) are a group of genetic disease with an autosomal recessive inheritance caused by a defect in glycosylation (Freeze HH et al. 2017).

CDG are divided in two main groups: CDG1 (Figure 8) and CDG2 (Figure 9). The first one is characterised by a general hypoglycosylation status of proteins due to defects on glycan precursor assemblage. The second one has an alteration of glycan composition because mutations are situated on genes codifying glycosyltransferases and membrane-nucleotide sugar transporters. CDG-N-linked are disorders caused by the defective synthesis of N-glycans with an early infancy outbreak.

Because the glycosylation has effect on many proteins that have a different function, CDGs have disparate symptoms. In the 70% of all known case (CDG-1A), the defective enzyme is the phosphomannomutase-2 (PMM2). The disease causes a developmental delay that can lead to mental disability. It impairs the ability to both move and coordinate the movements. Approximately 20% of cases with the disease die within the first year of life. CDG-1A patients have a decrease in motor-nerve conduction velocity, but less noticeable effects on sensory nerve conduction, indicating the presence of a PNS neuropathy (Pascual-Castroviejo I et al. 2006) and suggesting an important role of N-linked glycans in PNS physiology.

Mutations also in other genes involved in glycan biosynthesis have been also related to the onset of PNS neurodegenerative diseases. For instance, GlcNAcT-I inactivation, a Golgi glycosyltransferase essential for the biosynthesis of hybrid and complex N-glycans, was found to be responsible for severe neuropathies leading to tremors and paralysis (Scott H et al. 2014; Ye Z et al. 2004).

The number of mutations affecting the genes involved in the glycan formation is constantly increasing, thus studies of CDG patients can also provide useful information about the role of specific glycans in the PNS myelin function.

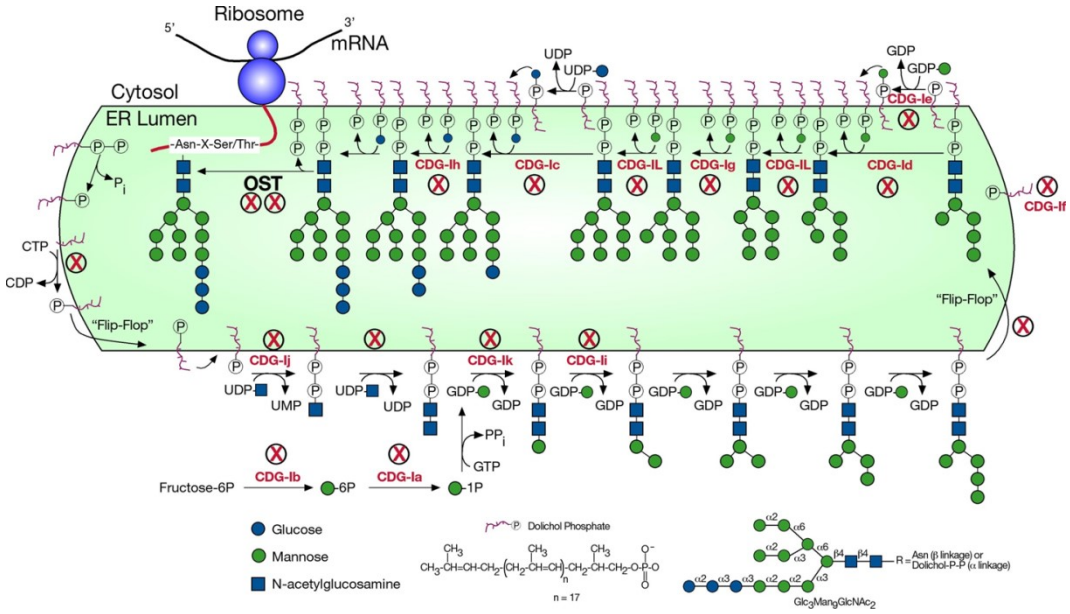

Figure 8. Location of defects in type I congenital disorders of glycosylation (CDG-I) (Freeze HH et al. 2009)

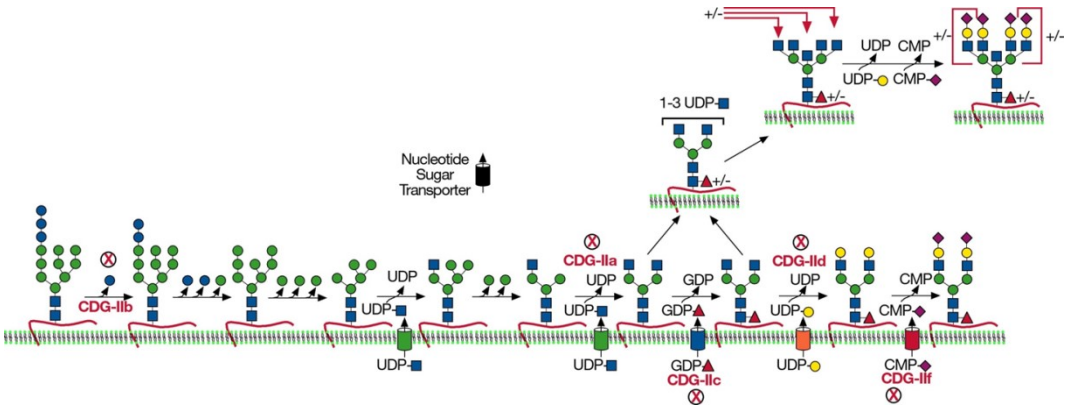

Figure 9. Location of defects in type II congenital disorders of glycosylation (CDG-II) (Freeze HH et al. 2009)

1.2.3 MPZ N-glycosylation

As indicated above, MPZ exhibits a single N-linked glycosylation site (N122) and it represents the most abundant protein carrying N-linked glycans in PNS myelin (Figure 10). Thus, its glycans accounts for the majority myelin glycosylation. Recently, several spontaneous human mutations that modify the glycosylation status of MPZ have been identified, either by abrogating the single glycosylation site or by adding new sites for N-linked glycosylation (Prada V et al. 2012; Grandis M et al. 2008). Altogether, clinical data from patients suggest that MPZ glycosylation status is important to maintain correct myelin function in PNS.

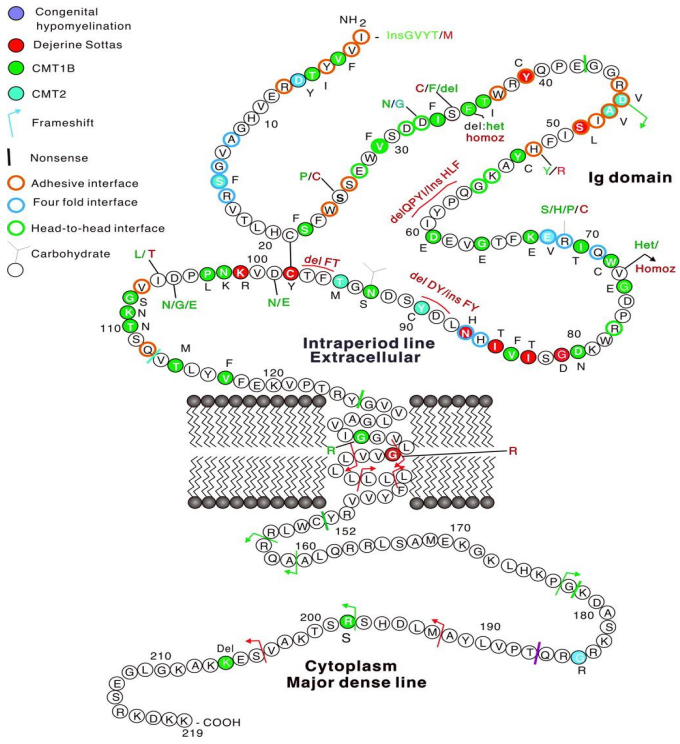

Figure 10. Representation of MPZ. Mutations highlighted in different colour lead to different form of CMT. (Shy ME et al. 2004)

These results are also confirmed by *in vitro* experiments, which demonstrated that glycosylation is essential for the adhesive properties of

MPZ (Filbin MT et al. 2007). Recent evidences have demonstrated that in mice loss of sulfatation of N-linked glycans induces abnormal myelination and axonal degeneration of PNS (Yoshimura T et al. 2017).

Occurrence of age-dependent alterations in MPZ glycans in the peripheral nerve and mammalian spinal cord have been reported, suggesting that the glycan heterogeneity might be regulated by alterations in physiological conditions, although details of the structural changes of the carbohydrate chains have not been elucidated yet (Sato Y et al. 2000, 1999). Interestingly, rat MPZ oligosaccharides were reported to change during development, with a prevalence of endo-H resistant N-linked glycans after birth, which are converted to endo-H sensitive glycans in adult animals (Brunden KR 1992). The endo-H sensitive glycans were suggested to be of hybrid type, due to their inability to interact with *Galanthus nivalis* agglutinin (Brunden KR 1992). Moreover, significant alterations in MPZ glycan structures have been reported after rat nerve resection or crushing (Rotenstein L et al. 2008).

Detailed structures of N-linked glycans of MPZ were recently obtained by mass spectrometry, from shark, frog and bovine myelin (Rotenstein L et al. 2008; Xie B et al. 2007; Gallego RG 2001). Very recently, N-glycan structures were obtained also for rodents and porcine PNS myelin using DEAE-HPLC (Diethylaminoethanol–High Performance Liquid Chromatography) (Yoshimura T et al. 2017). The results pointed out important differences among evolutionary distant species. Oligosaccharides from bovine and porcine myelin are characterized by the presence of the HNK-1 (Human Natural Killer-1) and 6-*O*-sulfosialyl-Lewis X epitopes, together with other unusual sulfated structures (Yoshimura T et al. 2017; Voshol H 1996). HNK-1 is also the antigen recognized by auto-antibodies in some types of acquired human autoimmune neuropathies (Burger D et al.1992, 1990) (Figure 11).

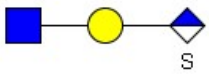

Figure 11. Representation of the HNK-1 epitope. GlcNAc-Gal-GlcA-$SO3^-$ (Drawn with Glycoworkbench)

HNK-1 has been reported in PNS myelin of mouse origin, where it seems to be restricted only to myelin surrounding motor fibers and not present in sensory nerves (Löw K et al. 1994), even if its presence has not been confirmed (Yoshimura T et al. 2017). Conversely, antibodies recognizing this epitope are not able to stain both motor and sensitive fibers in rat PNS (Martini R 1998). These findings indicate that HNK-1 can have a different role depending on localization and that important differences exist between related species, posing questions about the function of this structure in myelin. Moreover, HNK-1 epitope also showed a developmental regulation and a different localization between region of compact and non-compact paranodal myelin (Field MC. et al. 1992).

As reported above, several studies have suggested or clearly identified N-linked hybrid structures as major component in adult compact myelin from different species. The presence of hybrid structure also on human myelin is not clear, since one report indicated the presence of complex type N-linked glycans only (Burger D et al. 1992), while a second report suggested the presence of hybrid structures (Field MC et al. 1992). However, a detailed structural analysis is missing for human PNS myelin. Another important issue has been raised by the results of Fasano and co-workers, who analysed N-linked glycans from bovine MPZ purified from lipid rafts and in non-raft regions (Fasano A et al. 2008). A prevalence of hybrid oligosaccharides was observed in MPZ from lipid rafts, suggesting a role for this type of structures in MPZ targeting to specific membrane sites (Fasano A et al. 2008). Although myelin is a membrane characterized by

very specialized regions, the mechanisms that control protein targeting are not fully understood. Indeed, the D61N missense mutation of MPZ, which leads to a severe CMT1B syndrome and is characterized by the presence of an extra-site for N-linked glycosylation, also impairs intracellular trafficking of the protein, suggesting that glycosylation can affect MPZ localization (Prada V. et al. 2012).

1.2.4 Charcot-Marie Tooth diseases

Charcot-Marie-Tooth (CMT) disease comprises a large group of progressive disorders that affect peripheral nerves, due to mutations in many different genes, mostly inherited in an autosomal dominant pattern. CMT disease is the most common inherited disorder that involves the PNS and affects approximately 1 in 2,500 people. It concerns 50,000 people in the European Union and probably >2.6 million worldwide. CMT remains incurable and only supportive care is presently available (Pareyson D et al. 2017). It is characterized by degeneration of both myelin sheaths and axons of peripheral nerves, presenting a wide spectrum of severity of symptoms and anatomopathological findings (Pareyson D. et al. 2017).

CMT1 represent about 60% of patients who have demyelinating CMT. CMT1 is characterised by a slow nerve conduction and it is caused by mutations in genes expressed in myelinating Schwann cells. CMT1A is often caused by the duplication of PMP22 gene and usually patients present the “classical CMT phenotype”. The clinical onset is in the first 20 years; the main symptom is represented by difficulty on walking, caused by deformity of the lower limb. CMT1B accounts for 10% of total CMT1 diseases and it is caused by over 200 mutations in the MPZ gene. (Brennan KM et.al 2015).

CMT2 is clinically similar to CMT1, has relatively normal nerve conduction velocities with evidence of axonal degeneration. It is characterized by muscular atrophy and bland sensory loss. There are several subtypes with a common clinical phenotype that can be distinguished only by studying gene mutation (Bird TD et al. 1998).

CMT4 is autosomal recessive demyelinating CMT1 like, characterized by an early outbreak in the first years of life. It is a severe neuropathy, which cause spinal deformities and disability. (Brennan KM et.al 2015).

Several mouse transgenic models mimicking CMTs have been developed, representing powerful tools to study the molecular mechanisms at the basis of the disease and to develop possible therapeutic strategies. Table 1 reports a summary of the most frequent types of CMT diseases, including the mutated gene and the corresponding phenotype.

Type	Gene/locus	Specific phenotype
Autosomal dominant CMT1 (AD CMT1)		
CMT1A	Dup 17p (PMP22)	Classic CMT1
CMT1B	MPZ	CMT1/DSN/CHN/intermediate/CMT2
CMT1C	LITAF	Classic CMT1
CMT1D	EGR2	Classic CMT1/DSN/CHN
CMT1E	PMP22 (point mutation)	Classic CMT1/DSN/CHN
CMT1F	NEFL	CMT2 but can have slow MCVs in CMT1 range + 2 early onset severe disease
CMT1	FBLN5	CMT1/macular degeneration/hyperelastic skin
Hereditary neuropathy with liability to pressure palsies (HNPP)		
HNPP	Del 17p (PMP-22)	Typical HNPP
	PMP-22 (point mutation)	Typical HNPP
X-linked CMT		
CMT1X	GJβ1	Intermediate ± patchy MCVs/male MCVs, female MCVs
CMTX dominant	PDK3	Classic CMT1
CMTX recessive (Cowchock)	AIFM1	Axonal/infantile onset/learning difficulties
Autosomal recessive demyelinating (CMT4)		
CMT4A	GDAP1	CMT1 or CMT2 usually early onset and severe/vocal cord and diaphragm paralysis described/rare AD CMT2 families described
CMT4B1	MTMR2	Severe CMT1/facial/bulbar/focally folded myelin
CMT4B2	SBF2	Severe CMT1/glaucoma/focally folded myelin
CMT 4B3	SBF1	Severe CMT/scoliosis/syndactyly/focally folded myelin
CMT4C	SH3TC2	Severe CMT1/scoliosis/cytoplasmic expansions
CMT4D (HMSNL)	NDRG1	Severe CMT1/gypsy/deafness/tongue atrophy
CMT4E	EGR2	Classic CMT1/DSN/CHN
CMT4F	PRX	CMT1/more sensory/focally folded myelin
CMT4G	HK1	Severe CMT1
CMT4H	FGD4	Severe CMT1
CMT4J	FIG4	Severe CMT1 ± ALS phenotype in adulthood
CCFDN	CTDP1	CMT1/gypsy/cataracts/dysmorphic features
CMT4	SURF	CMT1 with nystagmus/ataxia
CMT1	PMP22 (point mutation)	Classic CMT1/DSN/CHN/HNPP
CMT1	MPZ	CMT1/DSN/CHN/intermediate/CMT2

AD – autosomal dominant; AR – autosomal recessive; CMT – Charcot–Marie–Tooth; DI – dominant intermediate; RI – recessive intermediate; CCFDN – congenital cataracts, facial dysmorphism, and neuropathy; dup – duplication; del – deletion; PMP22 – Peipheral myelin protein 22; MPZ – Myelin protein zero; LITAF – Lipopolysaccharide-induced tumor necrosis factor alpha; EGR2 – Early growth response-2; DSN – Déjèrine–Sottas neuropathy; CHN – Congenital hypomyelinating neuropathy; NEFL – neurofilament; FBLN5 – Fibulin-5; GJβ1 – Gap junction beta 1/Connexin 32; PDK3 – Pyruvate dehydrogenase kinase isoenzyme 3; AIFM1 – Apoptosis-inducing factor mitochondrion associated 1; GDAP1 – Ganglioside-induced differentiation-association protein 1; MTMR2 – Myotubularin-related protein-2; SBF2 – SET binding factor 2; SBF1 – SET binding factor 1; SH3TC2 – SH3 domain and tetratricopeptide repeat domain 2; NDRG1 – N-myc downstream regulated 1; PRX – Periaxin; FDG4 – Frabin; FIG4 – phosphoinositide phosphatase FIG4; CTDP1 – C-terminal domain of RNA polymerase II subunit A, phosphatase of, subunit 1; HK1 – Hexokinase 1; SURF1 – Surfeit-1 protein; ALS – amyotrophic lateral sclerosis.

Table 1. Chart showing CMT mutation and phenotype (Brennan KM et al. 2015)

1.3 Glycans structural analysis

1.3.1 Glycans and sugars derivatization

Sugar have a high number of functional groups, different tautomeric form and some of them are very labile, so glycans analysis can be difficult. For this reason, glycans usually undergo through different modification before being analysed. There are a lot of possible modification as reported in Table 2 and each has its own advantages/drawbacks. Therefore, it is important to choose the derivatization method that suits best to the analysis.

The alditol acetate procedure is a good method for sugar composition analysis of glycans by GC-MS and it consists in release of monosaccharides by acid hydrolysis followed by the reduction of the aldehyde or ketone group of the sugar and the subsequent acetylation of every hydroxyl group. This derivatization removes the anomeric centre of the sugar in order to give only one signal for each sugar in gas chromatography. The main drawback is that different sugars can lead to the same alditol. For example, fructose can be equally convert to glucitole or mannitole because the reduction of the ketonic group is not stereo specific.

The Partially Methylated Alditol Acetates (PMAA) is the best method and one of the only available for sugar linkage analysis. The procedure consists in a first permethylation step, that involves the addition of methyl groups (CH_3) to all of the hydroxyl and N-acetyl groups. Methyl also esterifies the carboxy function on the sialic acid. The modified glycans will then undergo the alditol acetate procedure, as described above. In this way, it is possible to identify the linkage of the glycans by analysis of the fragmentation spectra, since the hydroxyl groups that were involved in the glycosidic bond are now acetylated and all the hydroxyl that were free are

now methylated. (Ruiz-Matute AI et al. 2011; Hellerqvist CG 1990). (Figure 12)

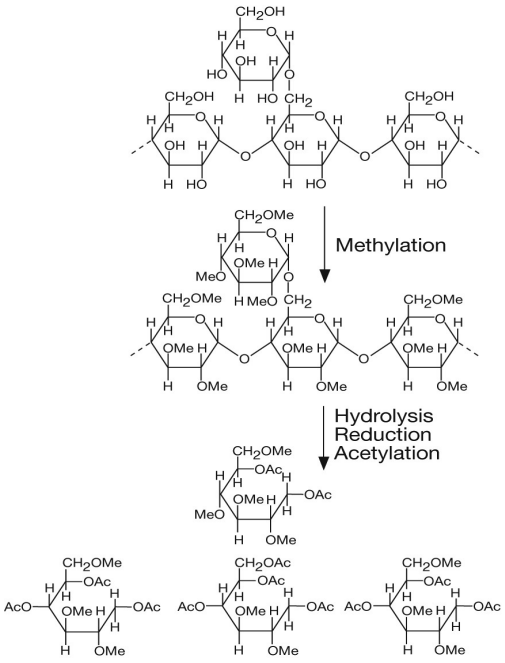

Figure 12. Derivatization of sugar for linkage analysis. The glycan is permethylated before acid hydrolysis and then acetylated. (Essentials of glycobiology, Second Edtion Chapter 47, figure 3)

The permethylation techniques that have been developed for PMAA analysis have been also successfully applied to MALDI-MS and ESI-MS analysis of glycans. Permethylation of glycans offers several advantages. For instance, by increasing glycan hydrophobicity, it allows also Liquid Chromatography–Mass Spectrometry (LC-MS) analysis. Moreover, since also the carboxy functional group of sialic acid is also methylated, losing the negative charge, both neutral and acidic glycans can be detected in positive ion mode using MALDI-TOF-MS. The protection of the hydroxyl group with a methyl group will also increase stability and the samples can be kept for months at room temperature. Methylation of the hydroxyl groups gives a better sensitivity and increase the hydrophobicity of the

sugars making easier to remove salts and polar contaminants with chromatographic methods.

Derivatives	Anomeric centre	Derivatization reaction	Advantages	Drawbacks
Methyl ethers	Non-modified (Multiple peaks)	ROH + CH_2–X → R–O–CH_3 + HX	- Suitable for analysis of low molecular weight carbohydrates and for structural analysis of polysaccharides	- Complex chromatograms due to the different tautomeric forms - Time-consuming preparation - Thermal degradation at high temperatures - Lack of good resolution in GC
Acetates	Non-modified (Multiple peaks)	ROH + Ac–X → R–O–Ac + HX	- Suitable for analysis of low molecular weight carbohydrates - Chemical and thermical stability	- Complex chromatograms due to the different tautomeric forms - Low volatility comparing to trimethylsilyl ethers
Trifluoroacetates	Non-modified (Multiple peaks)	ROH + CF_3CO–X → R–O–$COCF_3$ + HX	- More volatile than either acetates or trimethylsilyl ethers - Applicable to carbohydrates of a wide range of molecular weights - Allows the use of flower analysis temperatures	- Complex chromatograms due to the different tautomeric forms - Difficulty in achieving satisfactory quantitation
Trimethylsilyl ethers	Non-modified (Multiple peaks)	ROH + $(CH_3)_3$Si–X → R–O–Si$(CH_3)_3$ + HX	- More volatile, less polar and more thermally stable than methyl ethers and acetates - Rapid derivatization method which proceeds under mild conditions - Large number of silylating reagents available - Useful for quantifying equilibrium forms of carbohydrates in solution - Derivatives most widely utilized	- Complex chromatograms due to the different tautomeric forms. - Samples must be completely dried - Silylation reagents are moisture sensitive
Trimethylsilyl oximes	Modified (Two peaks)	(1) R–CHOH–CHO + NH_2OH → R–CHOH–C=NOH + H_2O (2) R–CHOH–C=NOH + $(CH_3)_3$Si–X → R–CHOSi$(CH_3)_3$–C=NO–Si$(CH_3)_3$ + HX	- Decreases the number of chromatographic peaks of reducing carbohydrates to *anti* (*E*) and *syn* (*Z*) isomers - Applicable to both aldoses and ketoses	- Samples must be totally dry - Derivatives are stable for a long time
Trimethylsilyl alkyl oximes	Modified (Two peaks)	(1) R–CHOH–CHO + NH_2OR′ → R–CHOH–C=NOR′ + H_2O (2) R–CHOH–C=NOR′ + $(CH_3)_3$Si–X → R–CHOSi$(CH_3)_3$–C=NO–R′ + HX	- Decreases the number of chromatographic peaks of reducing carbohydrates to *anti* (*E*) and *syn* (*Z*) isomers - Applicable to both aldoses and ketoses	- Samples must be totally dry
Alditol acetates	Modified (One peak)	(1) R–CHOH–CHO + $NaBH_4$ → R–CHOH–CH_2OH (2) R–CHOH–CH_2OH + Ac–X → R–CHOAc–CH_2O–Ac + HX	- Elimination of the anomeric centre giving one chromatographic peak for each aldose - Very stable compounds - Used for sugar composition analysis of macromolecules - Allows separation of complex mixtures	- Different sugars can lead to the same alditol - Each ketose yields a mixture of two alditols - Frequently, tedious and time-consuming derivatization procedure - Reaction products (acid by-products) often need to be removed before analysis - Acylation reagents are moisture sensitive
Aldononitrile acetates	Modified (One peak)	(1) R–CHOH–CHO + NH_2OH → R–CHOH–C=NOH + H_2O (2) R–CHOH–C=NOH + Ac–X → R–CHOAc–C≡N + HX	- Give only one product for each aldose - Water does not interfere with the reaction	- Formation of non-volatile products for ketoses - Non-appropriate for GC analyses of real samples where aldoses and ketoses exist simultaneously
Dialkyl dithioacetals	Modified (One peak)	(1) R–CHOH–CHO + R′–SH → R–CHOH–CH(S–R′)$_2$ + H_2O (2) R–CHOH–CH(S–R′)$_2$ + $(CH_3)_3$Si–X → R–CHOSi$(CH_3)_3$–CH(S–R′)$_2$	- Form a single peak for each aldose - Stable products	- Difficulties in the preparation procedure basically related to the use of a thiol as regent of derivatization - Variable yields are obtained - In some cases, formation of byproducts contaminating the chromatographic system

Table 2. Table showing different sugar derivatization method underlining advantages and drawbacks (Ruiz-Matute AI et al. 2011)

1.3.2 Mass spectrometry analyses and ionization techniques

The most commonly used instruments to study glycans in mass spectrometry, and in general biopolymers, are Matrix-Assisted Laser Desorption/Ionization Time-of-flight Mass Spectrometry (MALDI-TOF MS) and Electrospray Ionization- Mass Spectrometry (ESI-MS).

In MALDI, as the name suggests, the ionization is assisted by a matrix that absorb the laser energy and help to ionize the molecule mixed together. In this way can be observed even analytes that are very difficult to ionize. MALDI has the advantage that data are obtained with minimal sample concentration and it is very tolerant with salts contamination. The main drawback is that there is a significant degree of fragmentation when negative glycan substituents, like sialic acid, sulfate, and phosphate groups are present (Zaia J 2010). For this reason, it is better to analyse permethylated glycans that are considerably more stable than their native counterparts avoiding the risk of fragmentation during the MALDI ionization.

Another ionization source that can be used is Electrospray Ionization (ESI), in which a high voltage is applied to a liquid in a small capillary creating an aerosol. ESI has the advantage to be able to analyse native acidic glycans without glycans fragmentation and usually the signals are better resolved because the absence of matrix adduct peaks. On the other hand, the spectra are more complex due the different charge state and the sample must be free of salts.

1.3.3 MALDI TOF matrix choice

The first step before proceeding with a MALDI analysis is the matrix choice. The sample has to be co-crystallized on a MALDI metal plate with a large excess of matrix in order to be analysed with this technique. Laser irradiation of the matrix induces electronic excitation of the matrix molecules. This cause desorption of the analytes and matrix ions from the surface of the crystal to be analysed and by the mass spectrometer in the positive or negative ion mode, in an appropriate m/z range.

There are different matrices suitable for MALDI analysis and the choice will depend on the molecule to be analysed. For example, the most common matrix to analyse peptide is the alpha-cyano-4-hydroxycinnamic acid that give good results with peptides and small molecule in general, but is less indicated than sinapinic acid in the case of proteins. In particular, glycans are usually analysed with two different matrices: the 2,5-dihydroxybenzoic acid (DHB) and 3,4-diaminobenzophenone (DABP). Both can be used with good results, but some studies (Khoo K-H et al. 2010) suggest that DHB is in general better for detecting glycans in the positive ion mode, instead DABP gives the best sensitivity for detecting permethylated sulfated glycans in negative ion mode.

1.3.4 MALDI TOF analysis of glycans

The preparation of sample for MALDI require mixing of the sample with an acidic matrix and drying a microliter volume on a MALDI plate, to allow the formation of crystals. When hit by the pulsed laser beam, the matrix absorbs the energy of the UV light; the top surface of the dried drop heats and a small part is vaporized, carrying intact ionized glycans.

As already mentioned above, the mass spectrometer can be set in the positive or negative ions for analysis. In the case of permethylated glycan it is suggested to perform the analysis in positive ion mode, because the sialylated species are no more negatively charged. Even mono sulphated glycans give good results in positive mode. The ionized glycans are then accelerated by an electric field and the time that each ion need to reach the detector will depend on the mass-to-charge ratio. The instrument then determines the mass-to-charge ratio via time measurement. The most commonly used detector to measure the time of flight is the electron multiplier, which consists in continuous or discontinuous dynodes series. When a charged particle hits the first dynode, it produces the emission of several electrons, which are then attracted to a second dynode and the process can continue on cascade amplifying the signal, in order to produce an electric current that can be read by the electronic system.

The final spectra of the MALDI TOF analysis contains different peaks in a particular m/z range each of which correspond to a different glycan. Structures are assigned to each peak in the MALDI "fingerprinting", which is based on the glycan composition (given by an m/z value) and the knowledge of the glycans biosynthetic pathways. Then it is possible to confirm the structure with MS/MS analysis.

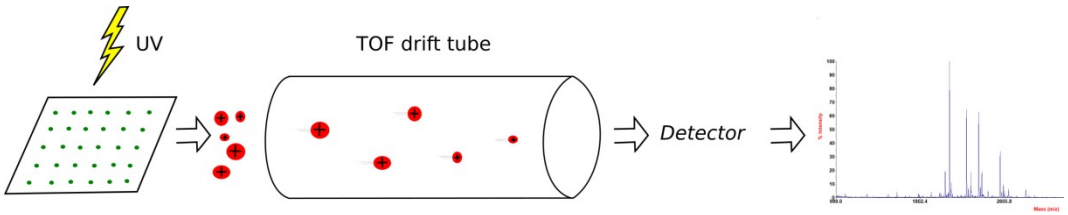

Figure 13. Diagram showing the steps of a MALDI TOF analysis

There are general rules to determine the molecular weight of a glycan, which are depicted in Figure 14. As shown in the figure, when calculating the molecular weight, it is important to consider the contribution of each monosaccharide and its substituents, as it is the case for methyl groups. Moreover, Figure 14 also shows that the method used for glycan release can have an important effect: for N-linked glycans, which are released by means of PNGase, the aldehyde group at reducing end is retained. On the contrary, for O-linked glycans the β-elimination procedure leads to the reduction of the aldehyde group of the first monosaccharide and the subsequent permethylation. This modification must be considered during mass spectra interpretation.

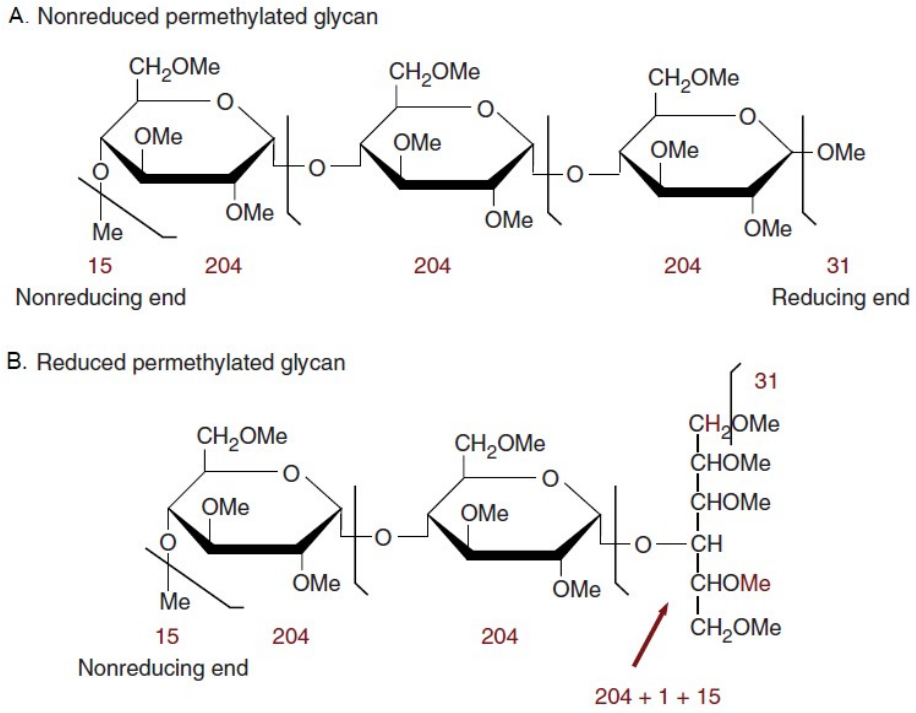

Figure 14. The molecular weight of the permethylated glycans can be obtained by considering the sugars composition and the permethylated mass ends. **A.** N-Glycan released with PNGase F follow the general rule: total sum of Permethylated Residues Mass + 46 + Na^+, where 46 represent the weight of the permethylated mass ends. **B.** For the O-glycans, reductive elimination leaves a free anomeric carbon and an additional site of permethylation on C5, so the resulting mass will be total sum of Permethylated Residues mass + 62 + Na^+. (Morelle W et al. 2007)

A chart reporting the mass of the permethylated monosaccharides that are found in human glycoproteins and the corresponding symbols that are used to depict glycan structures is reported in Figure 15.

Monosaccharide	Symbol	Permethylated Residue Mass (m.u.)
Deoxyhexose	▲ Fucose (Fuc)	174
Hexose	● Galactose (Gal) ● Mannose (Man)	204
N-acetylhexosamine	■ N- acetylglucosamine (GlcNAc)	245
Sialic acid	◆ N-acetylneuraminic acid (NeuAc) ◇ N-glycolylneuraminic acid (NeuGc)	361 391

Figure 15. The symbols used to illustrate glycan structures and the molecular mass contribution of each monosaccharide to the final mass of a permethylated glycans.

1.3.5 MALDI TOF/TOF analysis

In MALDI TOF/TOF ions are desorbed and ionized from the MALDI plate and then accelerated in the first TOF analyzer. Here, fragments continue to travel with the same velocity of the parent ion. At the end of the first TOF, only the ions of the selected mass and the derived fragments can pass to the second TOF. In the second TOF, the ions are accelerated, but this time fragments and parent ion will be separated and their time of arrival on the detector will be different (Pusch W et al. 2003).

This technique can be used to understand glycans composition starting from the m/z value of the parent ion and its fragments. For example, it is possible that different structures have the same m/z value, since mass gives no information about the sugar sequence or the type of linkage. Moreover, most sugars found in glycoproteins are isomers (GlcNAc- GalNAc) or epimers (Man-Gal). To overcome this problem, it is possible to use MS/MS fragmentation spectra to establish the structure of a glycan. Indeed, MS/MS is able to distinguish different glycans in most of the case, because it gives information about the fragmentation that can be different despite the same sugar monomer composition and the same mass. In this way, it is also possible to resolve different species that in MALDI-TOF analysis are represented by the same peak and to determine the relative abundance of each one.

In detail, the analysis is based on the knowledge of the glycans biosynthetic pathway, which depends on the organism and tissue, and the mass of the sugar monomer. An example is shown in Figure 16. Both the indicated structures have a molecular weight of 2635.3. However, when the molecules are subjected to MS/MS, they produce different fragments, which have significantly different masses. Based on the fragments it is possible to assign unequivocally the glycan structure.

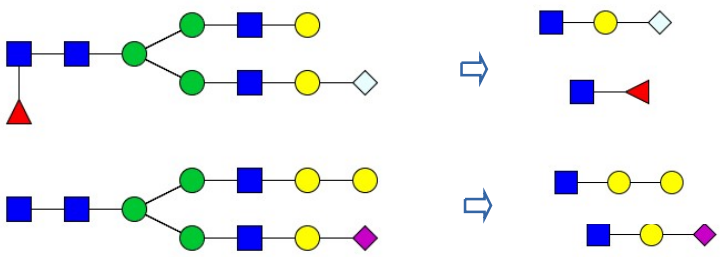

Figure 16. This image shows different glycans structure with the same molecular weight (2635.3 m.u.) but different fragments. (Drawn with Glycoworkbench)

Figure 17 reports an example of a MALDI-TOF MS/MS spectra of a permethylated glycan. The specie with 2360.1 m/z has been subjected to further fragmentation. Analysis of the generated fragments is consistent with and validate the proposed structure of the parent specie.

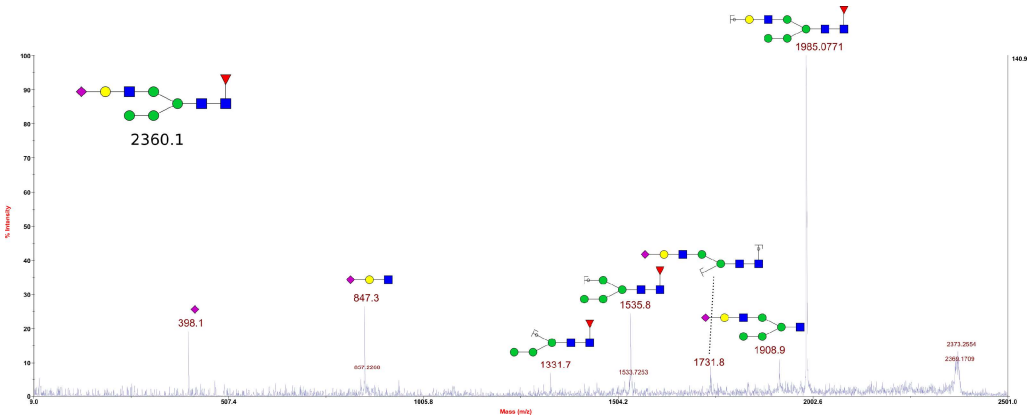

Figure 17. An example of MALDI TOF/TOF annotated spectra.

1.3.6 Glycoworkbench

GlycoWorkbench (Ceroni, A. 2008) provides an easy to use suite that allows a simpler identification of glycans by knowing the m/z values of the parent molecules and/or the fragmentation spectra. The editor gives an easy way to draw glycans, where it is possible to build sugar by sugar the complete structure. To calculate the correct molecular weight there are several options that consider possible modifications in order; in particular, it can be selected if the glycans are permethylated, with a reducing end, a free end, with sodium charges and so on.

A very good feature is the peak finder, which is able to find possible glycans that match with a particular m/z. However, it is necessary to have a very good knowledge of glycans possible structures to limit the number of hits. For example, if looking for N-glycans it will be good to search only for glycans with the GlcNAc2Man3 core.

Another important tool is the fragmentation prediction, which can show a list of fragments for a given structure. This is helpful for tandem mass sequencing because, as evidenced by Figure 18, the software reports the m/z and the mass of each fragment, which can be compared with the data obtained from the MS/MS for a selected peak.

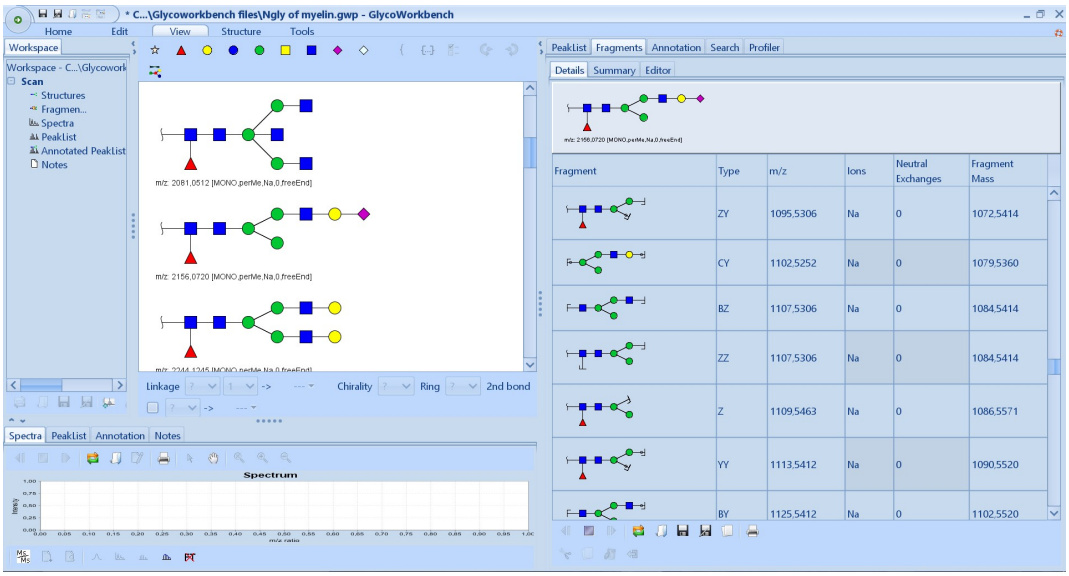

Figure 18. The working area of the Glycoworkbench suite: drawing, spectra trace, and fragment prediction.

1.4 Aim of the study

Modification of glycan structures is now recognized as a hallmark of several pathologic conditions, from inflammation to cancer and degenerative diseases. Altered glycosylation has been identified in several neurodegenerative diseases of the CNS (Kizuka Y et al. 2017). However, little information is presently available about the role of glycosylation in PNS pathologies.

Animal models represent an essential system to study the development and the physiopathology of the nervous system, due to the intrinsic difficulties for the use of samples of human origin (Martini R et al. 1997). For this reason, several transgenic and knock-out mice and rats or animals with spontaneous mutations have been established, mimicking hereditary human pathologies of PNS, such as CMT and related diseases.

However, it remains difficult to work with mice as animal models of the neurodegenerative diseases since the extremely limited amount of myelin that can be recovered from peripheral nerves in respect of CNS. Therefore, miniaturizing the process will help to acquire important data on animal models of diseases and to cut the cost of the animal facility.

The aim of this study will be focused on the optimisation of a method to perform a glycomic analysis, using MALDI-TOF mass spectrometry, from a very small amount of tissue from the peripheral nervous system of mice.

Materials and Methods

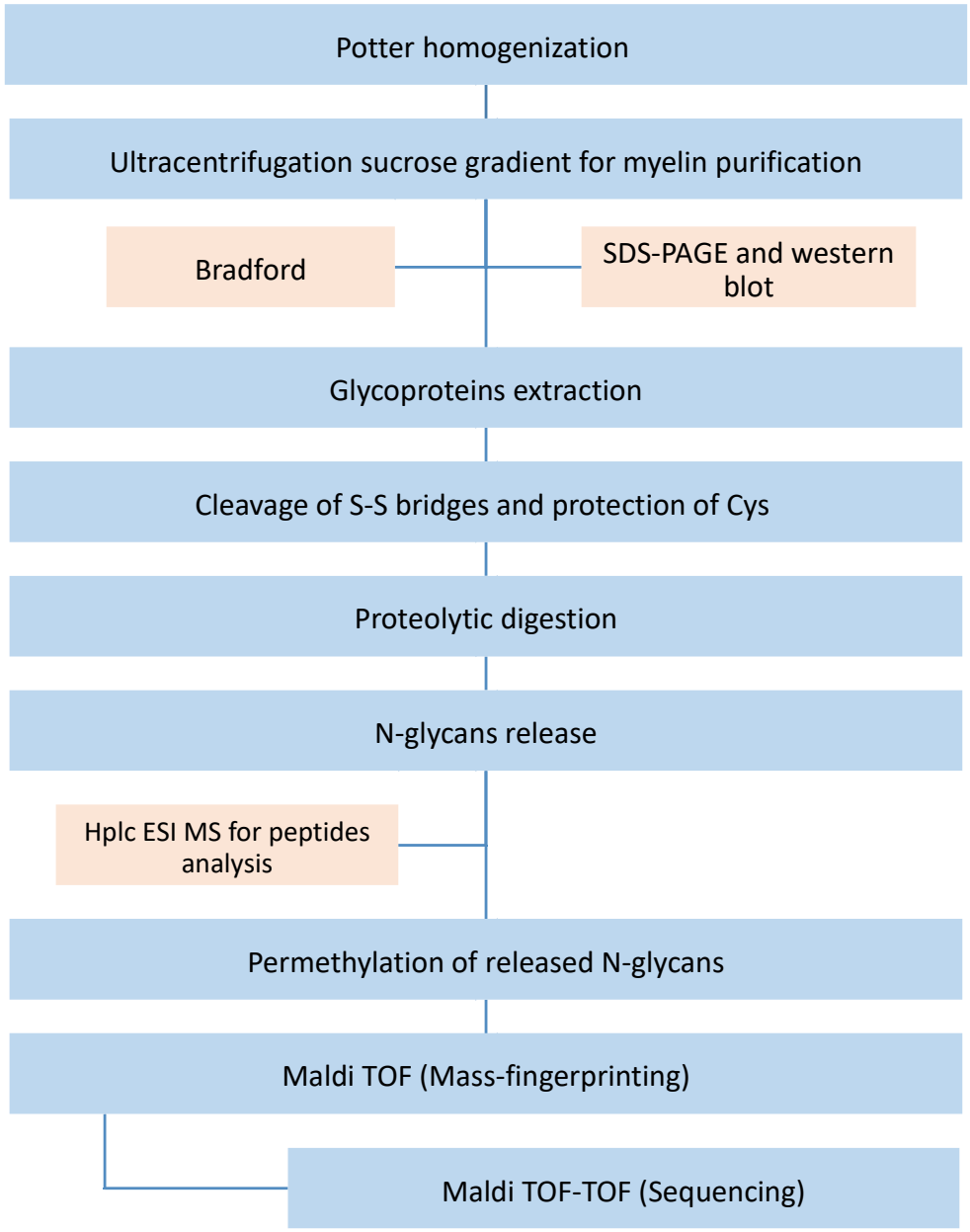

Figure 19. Overall procedure for the preparation and analysis of glycans from biological samples.

2.1 Myelin purification from C57BL mice sciatic nerves.

2.1.1 Myelin homogenization and ultracentrifugation

C57b mice were maintained and used at the animal facility of CBA-San Martino Hospital, Genova, following the international rules for experimental animal welfare and experimentations were approved by the internal ethical committee. Sciatic nerves were obtained from WT control mice used for other experiments. Nerve were collected immediately after animal sacrifice and snap frozen in liquid nitrogen. They were then stored at -80°C until processed.

Myelin can be enriched from homogenized sciatic nerves by sucrose gradient centrifugation, as the low-density membranes tend to accumulate in the interphase between 0.32 and 0.85 M sucrose. This method was initially proposed by Norton and colleagues (Norton WT. et al. 1973). Sciatic nerves from C57b mice (16 to 7 animals) were homogenized in buffer A (0,32 M sucrose, 10 µl of Protease Inhibitor Cocktails (PIC) [Sigma P8340-1ML], 2 mM EGTA) with Potter-Elveheim homogenizer. Different experiments proved that the best ratio to achieve a good purification is 1:20 between sample weight and solution. The centrifugation tube was initially filled with buffer B (0,85 M sucrose, 10 µl PIC, 2 mM EGTA) and the homogenate was then carefully layered on top of buffer B. The ratio of buffer A and buffer B must be 1:1. The tube was centrifuged with a TL-100 Beckmann® for 30 minutes at 4°C at 75,000 x g. The sucrose interphase was collected with a Pasteur pipette and placed into a clean tube. At this step, myelin membranes should be visible as a whitish cloud. It is possible that some contaminants can remain trapped in the

interphase layer, but nuclei and mitochondria are generally mostly found in the pellet of the gradient. To get rid of the remaining membrane contaminants, an osmotic shock in Milli-Q water was performed: the tube containing the recovered interphase was filled with water and incubated on ice for 10 minutes. The sample was then centrifuged for 15 minutes at 4°C at 75,000 x g. The pellet containing myelin was then resuspended again with 2 ml of Milli-Q water and centrifuged for 15 minutes at 4°C at 75,000 x g. The washed pellet from the last step containing myelin can be preserved at -20°C dry or in a water solution for few days.

2.1.2 SDS-PAGE and western blot

The protein concentration in the purified myelin was estimated using the Bradford assay. To follow the purification steps, the different fractions obtained after centrifugation were analysed by a 10% acrylamide SDS-PAGE, followed by Coomassie staining. A parallel SDS-PAGE was used for Western blot analysis. The separated proteins were transferred to a nitrocellulose membrane (Bio-Rad) by blotting overnight at 90 mA at 4°C in blot buffer (25 mM TRIS, 0.38 mM Glycine, 20% methanol, 0.1% SDS). Next, the membrane was blocked in 5% milk powder solution in PBS/ 0.1% Tween20 for 1 hour. The primary antibody anti-Myelin Protein Zero (ab31851, abcam) was used diluted 1:4000. After three washes with PBS/0.1% Tween to eliminate non-specific binding, the membrane was incubated with a secondary antibody (α-mouse conjugated with HRP, Santa Cruz Biotechnology). Detection was performed by a chemiluminescent method (ECL-GE Healthcare) using a ChemiDoc (Bio-Rad).

2.2 Glycans purification from myelin

2.2.1 Glycoprotein extraction

For glycoprotein extraction, the Folch chloroform-methanol method was used. Before starting with the sonication step, the sonicator probe was extensively washed with methanol and chloroform solution to avoid contamination. The myelin enriched sample was transferred to a clean 15 ml falcon tube, and the final sample volume was brought to 2 ml with Milli-Q water so that would be easier the to facilitate the sonication. The sample was sonicated in continuous mode at 40 Amps for 10 seconds followed by 2-3 minutes on ice and this process was repeated for 5 times.

Under fume hood, 2.67 volumes of methanol were added to the homogenate and mixed vigorously; then, 1.33 volumes of chloroform were added and the homogenate was vortexed. The sample was centrifuged for 10 min at 3000 rpm (in a tabletop centrifuge) to pellet proteins. However, the proteins stayed in the interphase instead of precipitate, so was necessary to remove the top aqueous layer, containing salts and nucleic acids, and add methanol to complete the precipitation (Wessel, D et al. 1984).

Specifically, the upper phase was carefully removed without disturbing the interphase and another 1 ml of methanol was added. The sample was centrifuged again for 10 min at 3000 rpm. After this second centrifugation, the proteins precipitated in the pellet, which was collected and dried under nitrogen to remove excess of chloroform/methanol.

2.2.2 Reduction, carboxymethylation and trypsin digestion

The pellet containing the precipitated proteins sample was resuspended in 0.5 ml of a DTT solution (DTT 2 mg/ml in degassed Tris/HCl 0.6 M pH 8.5), incubated for 60 min at 37°C and then briefly centrifuged to pull down the condensation. Then, 0.5 ml of iodoacetic acid (IAA) solution (12 mg/ml) were added and the sample was incubated in the dark at room temperature for 90 min.

The glycoproteins sample was transferred to a high-quality dialysis tube (Slide-A-Lyzer™ cut-off 10k or SnakeSkin™ Dialysis Tubing cut-off 7k; Thermofisher) and sealed. The carboxymethylation reaction was terminated with by a 48 hours dialysis for 48 hours in AMBIC buffer (50 mM ammonium hydrogen carbonate pH 8.4), changing the buffer regularly 4-5 times/day.

The dialysed sample was transferred into a 15 ml Falcon tube with a Pasteur pipette and, after the addition of 20 μg of trypsin (porcine T0303, Sigma), it was incubated for 24 h at 37°C. It was not necessary to stop the reaction since an unprotected trypsin, which undergoes through autolysis, was used.

Three drops of 5% acetic acid were added to the glycopeptides solution to lower the pH for the further Sep-Pak® purification. An Oasis HLB Plus® cartridge was attached to a 5-ml glass syringe and conditioned with the sequential addition of 5 ml of methanol, 5% acetic acid, 100% propanol and 15 ml of 5% acetic acid.

The sample was loaded using a plastic syringe, then the cartridge was washed with 5 ml of 5% acetic acid. Sequential elutions were done with 4 ml of 20 % propanol, 40% propanol, and 100% propanol. The three fractions were pooled together in a Corning glass tube and the volume was reduced with using a SpeedVac. All the collected fractions were combined

in the 20% propanol tube. The sample was finally lyophilised in a freeze-dryer.

2.2.3 N-glycans release

The lyophilised sample was resuspended in 250 µl of AMBIC buffer containing 5 U of N-glycosidase F and incubated at 37°C for 24 h. A second aliquot of the glycosidase was added after 8 hours. After the incubation, the sample was centrifuged.

The released N-linked glycans were separated from the mixture containing the residual peptides, using the same Sep-Pak® C18 method used after trypsin digestion. N-glycans were eluted from the cartridge using 5 ml of 5% acetic acid. The volume was reduced with SpeedVac and the sample was finally lyophilised in a freeze-dryer. The peptides and the O-linked glycopeptides were eluted using the three solutions with increasing propanol concentration, as described above. The eluted propanol fractions were pooled and, after volume reduction by Speed-vac, they were subjected to lyophilisation.

2.2.4 Dowex preparation and O-glycans release

To prepare 100 g of Dowex beads, 100 g of 50W X8, 50-100 mesh Dowex beads were added to 100 ml of 4 M HCl and left to decant. This wash was repeated twice more. Then beads were washed 15 times with Milli-Q water until the pH was stable at 6.5. Moreover, the beads were finally washed with 150 ml of 5% acetic acid and were left immersed in this solution. The beads can be stored in this solution for years.

A reducing solution (400 µl of 1,5 M KBH_4, 0,1 M KOH in Milli-Q water) was added in a Teflon-lined screw-capped tube (Corning) to the

lyophilised propanol fraction from the Sep-Pak® purification. The mixture was incubated for 14-16 hours at 45°C. The reaction was terminated by adding 5 drops of acetic acid until the fizzing stops. A desalting column was assembled using a Pasteur pipette fitted with a bottom filter of glass wool and about 1 ml of Dowex beads upon. A silicone tube was placed at the tapered end to control the flow.

The Dowex column was conditioned with 15 ml of 5% acetic acid. Then the sample was loaded and the flow through was collected; the beads were further washed with 5 ml of 5% acetic acid and this second elution step was pooled with the preceding one. The volume was reduced with SpeedVac and the sample was then lyophilised in a freeze-dryer. To remove better the excess of borates, the sample was resuspended 4 times with 0.5 ml in methanol-acetic acid 9:1 and dried under a nitrogen stream at room temperature. To eliminate residual water, the sample was finally lyophilised again in a freeze-dryer.

2.2.5 HPLC ESI MS for peptides analysis

The analysis was done by the Biopolymer Mass Spectrometry unit, Imperial College London, and it was performed on a small volume of the O-glycopeptides fraction. The peptides were separated on a Pepmap C18 nanocapillary column (15 cm length, 75 mm internal diameter) fitted to a nano-HPLC system (LC Packings) connected to an ABI QSTAR Pulsar Hybrid LC/MS/MS system (Applied Biosystems/MDS Sciex). A gradient from 0.05 % (v/v) formic acid in 95.5 % (v/v) water/acetonitrile to 0.05 % (v/v) formic acid in 95.5 % (v/v) acetonitrile/water was employed. Data were analysed using the Analyst QS Software.

2.3 Glycans permethylation and purification

2.3.1 Glycans permethylation

Before starting this procedure (North S.J et al. 2010), the sample has to be dried. Anhydrous DMSO (3 ml) was added in a dry glass mortar to 5 pellets of NaOH; the pellets were crushed with a glass pestle until the formation of a slurry. This was done quickly to avoid excessive absorption of moisture. This amount of slurry is required for 2 samples, the N-linked and the O-linked released glycans; 1 ml of the slurry was transferred with a Pasteur pipette to the glycan sample and immediately 0,7 ml of methyl iodide were added using a Gilson pipetting device equipped with a plastic tip. The samples were vortexed and then shaken for 2h at 4°C (Khoo K-H et al. 2010). The reaction was quenched by slow additions of cold 5% acetic acid with constant shaking to lessen the effects of the highly exothermic reaction. The pH was checked with a pH indicator to ensure that the sample pH is neutral or slightly acidic.

At this point 1.5 ml of chloroform were added and the sample was mixed thoroughly and then settled to allow the formation of two layers. The upper aqueous layer, which contains the sulfated permethylated glycans, was removed and transferred into another clean tube ready for Sep-Pak purification.

The organic phase, containing the neutral glycans, was washed 4 times with 5 ml of ultra-pure water, using a table centrifuge; the sample was then dried under a gentle stream of nitrogen and kept dried at -80°C until the further purification step.

2.3.2 Purification of neutral permethylated samples by Sep-Pak® C18

The Sep-Pak® cartridge was conditioned by sequential washes with methanol (5 ml), ultra-pure water (5 ml), acetonitrile (5 ml) and ultra-pure water (15 ml). The sample obtained from the organic phase of the step above, containing the neutral glycans, was dissolved in first 100 µl of methanol, then 100 µl of water were added. The resuspended sample was loaded with a Pasteur pipette onto the Sep-Pak® Cartridge and washed stepwise with 5 ml of Milli-Q water and 3 ml of 15% acetonitrile.

The permethylated glycans were eluted with 3 ml of 35%, 50% and 75% acetonitrile/water solutions and all fractions were collected in different glass tubes. The volume was reduced by SpeedVac to about 1 ml or less before lyophilising with a freeze dryer. The purified permethylated glycans are stable and can be conserved at room temperature for months.

2.3.3 Purification of sulfated permethylated samples by Sep-Pak® C18

The Sep-Pak® cartridge was conditioned by sequential washes with methanol (5 ml), ultra-pure water (5 ml), acetonitrile (5 ml) and ultra-pure water (3x5 ml), as described above in the previous paragraph.

The aqueous fraction obtained after permethylation was loaded, with a Pasteur pipette, onto a plastic syringe (used only for loading onto the Sep-Pak®) and washed stepwise with 15 ml of Ultra-pure water and 3 ml of 10% acetonitrile. The permethylated glycans were eluted with 3 ml each of 25% and 50% acetonitrile/water solution and the two fractions were collected in different glass tubes.

The volume was reduced by SpeedVac® to about 1 ml or less before lyophilising with a freeze dryer. The sample can be conserved at room temperature for months and it is quite stable; however, the sulfate groups may be lost.

2.4 Sample preparation and MALDI Analysis

2.4.1 Sample preparation

The lyophilised sample was dissolved in 10 µl of methanol and vortexed. One µl was combined with 1 µl of DABP (3,4-diamino-benzophenone) matrix solution (10 mg/ml) and spotted on a MALDI plate. The procedure was repeated for all the lyophilised Sep-Pak® acetonitrile fractions. After spotting all the samples the MALDI plate was put under vacuum and dried.

2.4.2 Preparation of calibrant solution for MALDI analysis

For the MS analysis the calibration was done using a peptide calibrant (100 mg/ml of peptide/protein mix Calmix-leucine enkephalin, bradykinin (fragment-8), angiotensin I, ACTH fragment 1–17, ACTH fragment 18–39, ACTH fragment 7–38, ACTH fragment 1–39 and insulin (bovine pancreas) in 0,1% TFA water).

For the MS/MS analysis a different peptide calibration solution was used consisting in: 1 pmol/ml solution of [Glu1]-fibrinopeptide B in 1:3 (v/v) acetonitrile/5% acetic acid (v/v).

The matrix used for peptides calibrants was composed by 10 mg/ml alpha-cyano-4-hydroxycinnamic acid in 50% acetonitrile in 0.1% (v/v) TFA in water)

2.4.3 MALDI TOF Mass-fingerprinting

MS data were acquired using a 4800 MALDI-TOF/TOF (Applied Biosystems) mass spectrometer. For the calibration, as described above, a laser intensity of 2200 was used and a 50 shots/spectrum were recorded. The calibration was done after accumulation of three spectra. The analysis was done in positive ion mode for the neutral permethylated N-glycans and in negative/positive ion mode for the sulfated N-glycans.

For the MALDI-TOF fingerprinting were used the following parameters:

-Laser intensity: 3500, Positive reflectron, with delayed extraction

-Mass range: m/z 500–5000,

-Low mass gate: m/z 500,

-Accelerating volts: 20 kV,

-Grid: 60–78%,

-Delay time: 220–280 ns.

2.4.4 MALDI TOF-TOF sequencing

MS/MS data were acquired using a 4800 MALDI-TOF/TOF (Applied Biosystems) mass spectrometer and the collision gas used was Argon. The system was calibrated with the peptides calibrant solution and then was ready to be used.

For the MALDI-TOF TOF sequencing were used the following parameters:

-mode: Positive reflectron, with metastable ion suppression

-laser intensity: 5000–6000

-shots: 1000 shots/spectrum, accumulate 10 spectra,

-mass range: m/z 50–5000,

-accelerating volts: 20 kV,

-Source-collision

-cell potential difference: 1 kV,

-CID: On, CID gas type: Inlet 1—Medium weight, Collision gas: Argon

-Collision gas pressure: 10, 4 mbar.

2.4.5 Data Analysis

MALDI Data were analysed using Data Explorer 4.9 Software (Applied Biosystems). This software is able to read the raw format and show the mass spectrometer data in an easy graphic interface. It is possible to set a cut off for abundance peak recognition, smooth graphic and select m/z range to analyse even small peaks. Majors peaks were then annotated manually (GlycoWorkBench software) with their respective structure, which was then confirmed by MS/MS fragmentation analysis.

Results

3.1 Optimization of myelin enrichment method

This myelin enrichment protocol is based on the Norton WT et al. 1973. The first experiments were devoted to the optimization of myelin enrichment from very small amounts of starting material, i.e the mouse sciatic nerves. The Potter-Elvehjem homogenisation method, despite it requires a long time and effort, was the best method tried to homogenise the samples. During this procedure, an insoluble aggregate could form, probably composed of connective tissue, which could not be homogenised even by vortexing. To avoid this aggregate formation, a second procedure was tried: sciatic nerves were homogenised with an Eppendorf pestle after a snap freeze step. This last method was faster and easier, but the aggregate was even bigger, so it was necessary a further step of Potter-Elvehjem homogenisation to recover the sample.

The final protocol was set up using a volume of less 1 ml with a minimal tissue amount. The lowest amount of material that could be processed with this protocol was derived from sciatic nerves of seven 28-days old mice. Yield of material was maximized by adding a second 500 µl wash of the glass and Teflon surfaces. A TL100 Beckmann® Centrifuge was then used for fractionation: even if it has a fixed angle rotor, and not a swinging bucket as suggested in the published protocols, it was possible to obtain a clear separation of the interphase enriched in myelin membranes. When the starting nerve material is very low, the interphase containing myelin is still well visible in a 3 ml or smaller centrifugation tube, while it was difficult to notice in larger ones. The following steps, osmotic shock and further centrifugation, allowed the quantitative recovery of the myelin-enriched

fraction in the pellet. The yield of protein was quite consistent among the different purifications. This procedure was also applied to very small amounts of rat brain (100 mg), giving the same results (not shown).

For glycan analysis, the second gradient purification and osmotic shock suggested by some published protocols were omitted, because the results obtained in ESI/MS (see below Table 3) indicated a very low contamination by proteins from other cell types already after the first purification step. On the other hand, a second gradient purification caused a further loss in sample recovery.

The protein concentration in the myelin enriched sample was estimated by Bradford Assay; about ≈ 500 μg of myelin proteins were recovered from ≈ 100 mg of tissue. This yield from the gradient purification ensure a sufficient amount of material, since the protocol used for glycan purification is highly optimized and the MALDI-TOF analyser has a high sensitivity.

SDS-PAGE and Western blot have shown that, during the gradient purification, myelin proteins were highly enriched. Figure 20 shows that the washed interphase (PI) contains only few proteins, compared to the upper and lower phases of the gradient; the most abundant band has a molecular weight consistent with MPZ (27 kDa). This band was further confirmed to be MPZ by Western blot analysis with an α-MPZ specific antibody. All the high molecular weight proteins were not found in the washed interphase, indicating that purification was successful, as also confirmed by comparison of the SDS-PAGE pattern with the published ones (see Section 1.1.1 Figure 4). The purified interphase (PI) was then used for glycoproteins extraction.

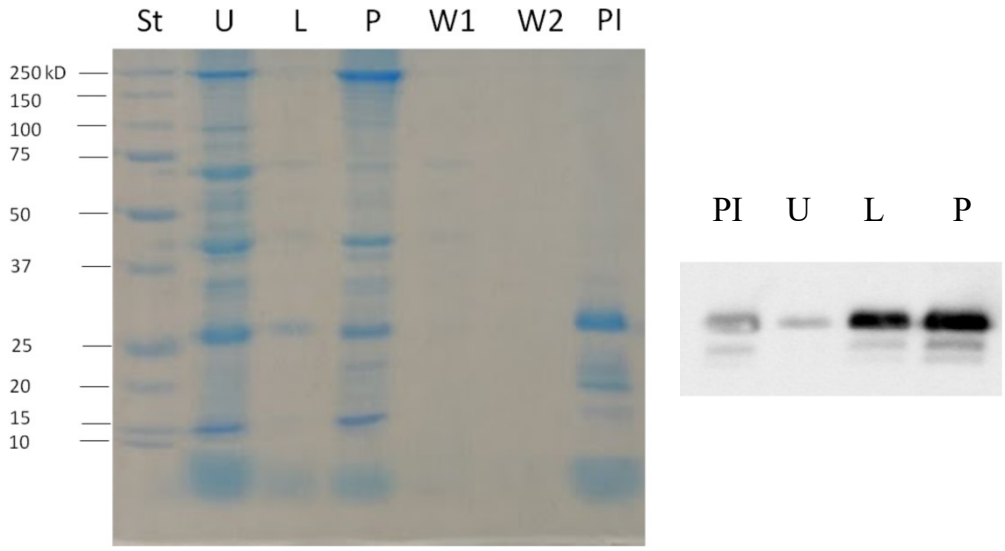

Figure 20. SDS-PAGE and Western blot (αMPZ) analysis of fractions obtained during myelin enrichment by sucrose gradient purification. St. molecular weight standards, U upper phase, L lower phase, P pellet, W1 Wash 1, W2 Wash 2, PI purified interphase.

ESI-MS proteomic analysis was used to confirm the identity of the purified proteins in the purified interphase enriched in myelin membranes. As shown in Table 3, besides porcine trypsin that was used for digestion, the most abundant peptides identified by ESI-MS were tubulin, MPZ, periaxin and MBP, all proteins typically found in compact myelin. No other contaminants were found at significant concentration. Among proteins that have high score hits, it is interesting to note that MPZ is the only glycosylated one. This suggests that the glycans are derived mainly from MPZ and this can be valuable to study glycans in MPZ associated pathologies. In the Supplemental Table 1 (ST1), all the peptides derived from MPZ that were found in the ESI/MS analysis are shown in detail. Moreover, all the peptide hits obtained by ESI/MS analysis are reported in Supplemental Table 2 (ST2).

Accession	Entry	mW (Da	PLGS Score	Pept ides	Theoret ical P	Coverage (%
TRYP_PIG	TRYP_PIG	24393	10794,42	9	14	25,1082
B2RSN3_MOUSE	Tubulin Beta chain	49920	4638,735	4	30	15,2809
MYP0_MOUSE	MPZ	27604	3947,008	8	18	30,2419
E9QQ57_MOUSE	Periaxin	147536	3938,486	52	85	39,7556
PRAX_MOUSE	Periaxin	147594	3689,903	52	86	38,9648
F6RT34_MOUSE	MBP	23182	2220,164	9	16	34,434
F6TYB7_MOUSE	MBP	21167	2195,693	10	17	40,8377
TBA1A_MOUSE	TBA1A	50103	2008,445	14	34	35,255
TBA1B_MOUSE	TBA1B	50119	1784,487	13	34	32,1508
TBA4A_MOUSE	TBA4A	49892	1026,153	9	34	29,0179

Table 3. Table showing the best hits of the ESI-MS Analysis. The full table can be found in the supplemental table 2 (**ST2**)

3.2 Optimization of glycans purification

Once the myelin has been purified, the next step is the optimization of the procedure from myelin-enriched sample to purified glycans.

The first passage is the glycoprotein extraction using the Folch Method, which consist in the precipitation of proteins with the concomitant removal of the lipid contaminants using methanol and chloroform. This method can be difficult operating with a small amount of sample; in this case, after centrifugation, proteins will tend to stay in the interphase instead of forming a precipitate. The best solution to avoid this problem was found in literature (Wessel, D et al. 1984) and consists in removing all the upper-phase above the sample, adding methanol and centrifuging again. In this way, proteins will precipitate at the bottom of the tube and will be ready for the next step of reduction and carboxymethylation.

The dialysis step to stop the reduction/carboxymethylation reaction was also improved by using Slide-A-Lyzer™ mini device. The original protocol suggested using SnakeSkin™, which is cheaper, but it can be difficult to handle and it has a large surface where proteins can bind and be lost. Slide-

A-Lyzer™ mini device offers the advantage of a quick buffer change and the possibility to keep the volume very small. In our conditions, this latter device proved to be significantly better over the SnakeSkin™ and no drawbacks were evidenced using Slide-A-Lyzer ™.

The main advantage to keep the volume small is that the sample can be dialysed in AMBIC, then directly transferred to a clean tube where trypsin can be directly added to start the proteolytic reaction. This modification avoids using SpeedVac or lyophilisation to reduce the volume after dialysis.

Another important consideration to maximise glycan recovery is to prefer a Freeze-drier to a SpeedVac to lyophilise the sample after the glycans release and purification step. If a SpeedVac is used, it will be very difficult to resuspend a completely dry sample without water and some glycans will be lost.

The entire procedure was repeated several times. Using 14 sciatic nerves from 28-days old mice, the main glycans peaks are still visible (data not shown). However, when very low concentration of proteins is handled, it is possible that the minimal contaminants in the sample, even at extremely low concentration, will prevail during the analysis, masking relevant signals and making difficult data interpretation. The most common contaminants that are very difficult to avoid are polyehyleneglycole and keratin. Therefore, extreme care must be used to avoid all possible contaminations, since the procedure is very repeatable and sensitive and contamination can represent the only one limiting factor.

3.3 Myelin glycoprofile of mice sciatic nerves

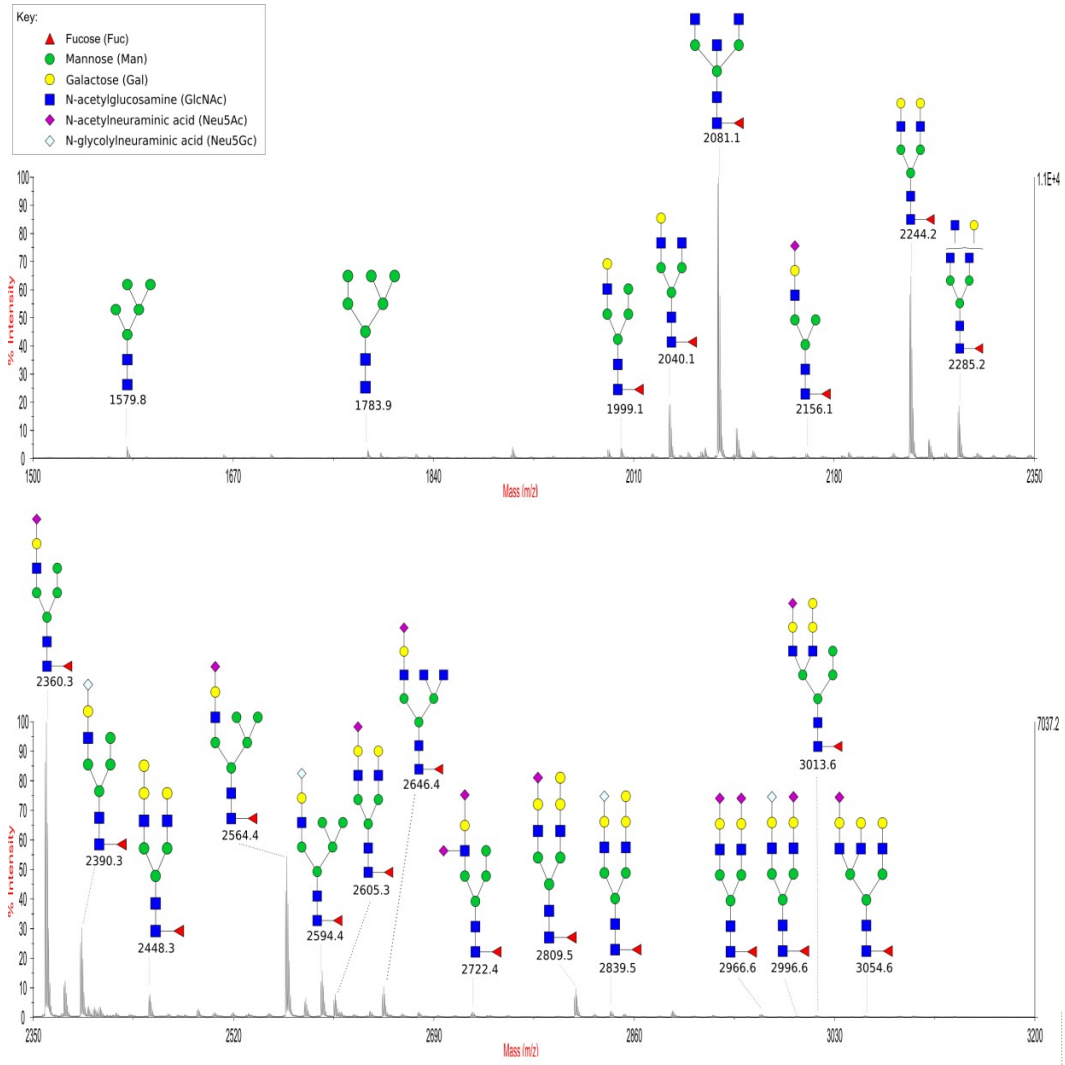

Figure 21. MALDI-TOF-MS profiles of permethylated *N*-glycans (50% Actonitrile fraction) derived from C57BL wild-type murine glycoproteins of myelin. All molecular ions are $[M + Na]^+$. The two panels cover sequential m/z ranges. Putative structures were obtained with MS-MS analysis and annotated according to the Consortium for Functional Glycomics (http://www.functionalglycomics.org) guidelines.

The purified glycans obtained from the different fractions after the last cartridge purification were then subjected to MALDI-TOF analysis. MALDI-MS analysis was used to determine the m/z of the different species. Based on the expected molecular weight, a possible glycan structure was proposed using the Glycoworkbench software. At this point, the putative structures were confirmed by MS/MS analysis, by evaluating the m/z generation of fragments from the parent molecule.

For neutral glycans, the fractions eluted from the Sep-Pack cartridge by 35% and 50% acetonitrile elution were both analysed. The MALDI-MS profiles found in both fractions were comparable, the only difference was that the 50 % shown a better abundance, in particular of glycan species at higher molecular mass.

Spectra of the 50% acetonitrile fraction are reported in Figure 21 and indicated the presence of neutral and sialylated N-linked glycans, mostly showing core fucosylated biantennary hybrid and complex structures. All the identified glycans are also summarized in Supplemental Table 3 (ST3). Both forms of sialic acid, the N-acetylneuraminic acid (Neu5Ac) and the N-glycolylneuraminic acid (Neu5Gc) are found, in agreement with the presence of both sialic acid forms in mammals, with the exclusion of humans (Varki A. 2010). The α-Gal epitope, typical of mammals excluding humans, consisting of two terminal galactose residues is also evidenced (Larsen RD 1990). Conversely, the HNK-1 epitope, which has been reported to be present in mouse PNS myelin (Löw K. et al. 1994), was not detected.

The polar permethylated glycans, containing the sulphated species, were eluted from the Sep-Pack cartridge using 25% and 50% acetonitrile. MALDI—TOF analysis was performed using both negative and positive mode. In negative ion mode, the spectra show only sulfated glycans, but with a low abundance. In positive ion mode, the analysis is more sensitive and it is possible to find also some neutral permethylated glycans.

Results of the 25 % fraction are reported in Figure 22 for negative mode and in Figure 23 for the positive mode. Both analyses provide similar results and reveal the presence of a high amount of mono-sulfated structures, which are indeed abundant in PNS myelin among mammals (Sedzik J et al. 2015). All the identified polar glycans are also summarized in Supplemental Table 4-5 (ST4, ST5).

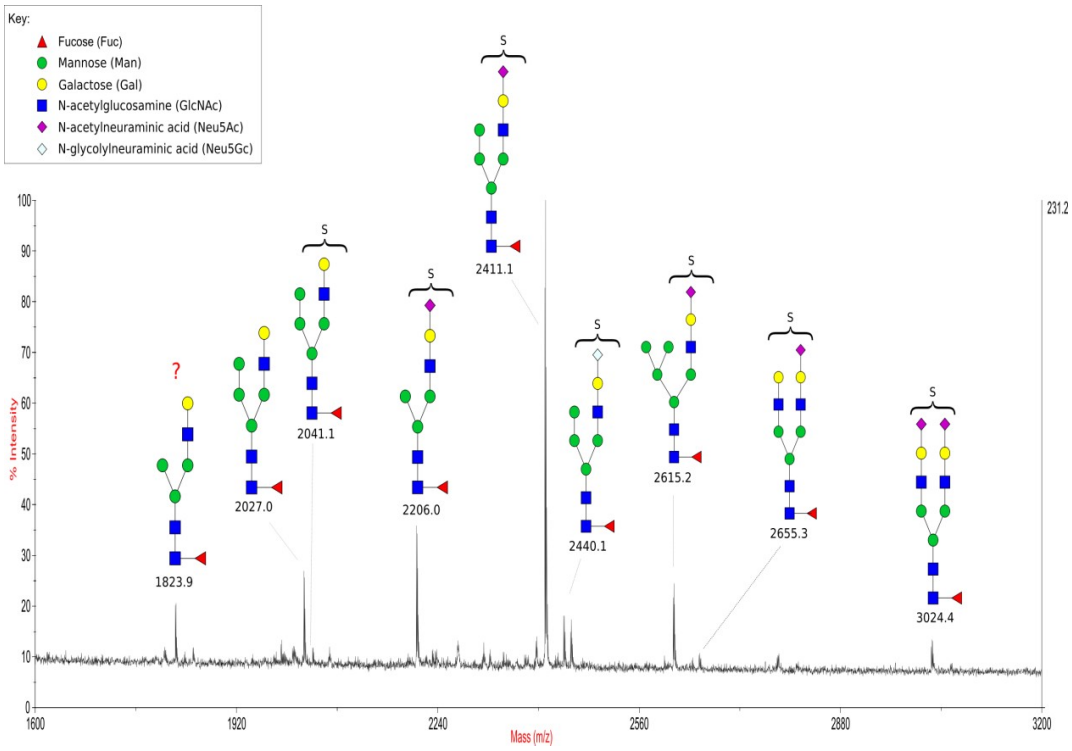

Figure 22. MALDI-TOF-MS profiles of permethylated sulfated N-glycans (25% acetonitrile fraction) derived from C57BL wild-type murine glycoproteins of myelin. All molecular ions are $[M-H]^-$.

Few low abundant species are found in the positive mode, which are not detected in the negative mode. It is interesting to note the presence also of a non-sulfated specie at 2399.1 m/z. This is because permethylated glycans can be found in the aqueous fraction if they have an incomplete permethylation. This happens because terminal sialic acid may form a salt bond with a Na^+, covering a site of permethylation on the sugar, so the glycans remain polar and stay in the aqueous phase. This happens when the

permethylation is done at 4°C; as consequence, in order to have a better evaluation of the abundance of sialylated sugar, it is always better to analyse both the chloroform and the aqueous fractions. Moreover, it is important to note that in these cases the glycans have a molecular weight 8 m.u. higher compared to the expected one, due to the presence of a sodium ion on the sialic acid (23 m.u.) instead of the methyl group (15 m.u) that was not inserted. In the Supplemental Figure 1 (SF1), there is an example of MALDI-MS/MS analysis, in which only the fragments with a sialic acid have a molecular weight 8 m.u. higher.

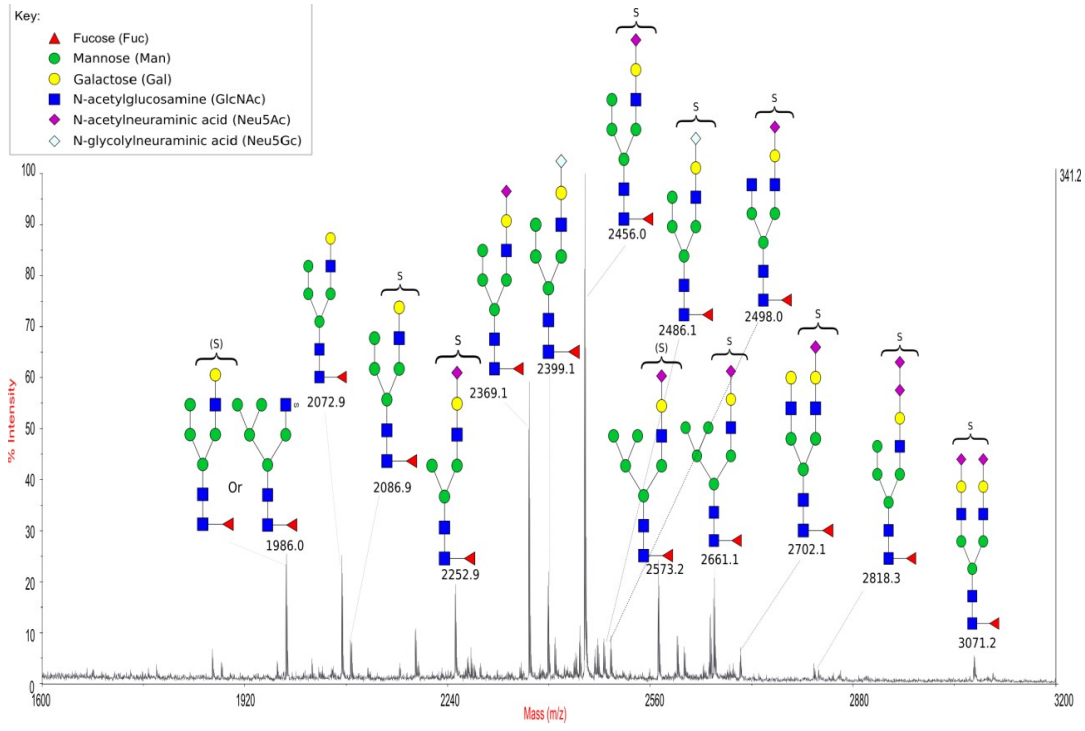

Figure 23. MALDI-TOF-MS profiles of permethylated sulfated N-glycans (25% acetonitrile fraction) derived from C57BL wild-type murine glycoproteins of myelin. Molecular ions completely permethylated are $[M + (n+1)Na\text{-}nH]^+$ where n is the number of sulfated group. The non-sulfated sialyl N-glycans have an incomplete permethylation on the terminal sialic acid and their resultant molecular ions are $[M + 2Na - CH_3]^+$

It is difficult to assign unequivocally the position of the sulfate group using MALDI-MS analysis; in particular, it was not possible to establish if the sulfate group was on the antennary galactose or N-acetylglucosamine, but this information need to be obtained using other methods. This represents a limitation of the MALDI-MS analysis done.

No other fractions obtained after cartridge purification of both the organic and aqueous phases revealed any glycans, as expected.

The samples obtained after β-elimination, Dowex purification and permethylation were also analysed for O-linked glycan presence. However, no significant amounts were found, at least for the amount of starting material used in our experimental conditions.

Discussion

Glycosylation is one of the most abundant form of post-translational modification of proteins. Many studies indicate that modifications of the glycosylation patterns either represent the basis for many diseases or can be signs underlying pathological conditions. However, glycosylation is often not considered enough, when studying pathogenetic mechanisms and the main reason is probably related to the difficulties of studying glycan structures.

One first difficulty is related to the macro- and micro-heterogeneity of glycans (Stanley P et al. 2009). Each molecule of the same protein produced in a single cell can harbour different glycan structures at the same glycosylation site. At the same time, a single specific protein can show different glycosylation profiles when produced in different cell types or tissues or in different moments during development or in pathological conditions, such as neoplastic transformation. Indeed, aberrant glycosylation is considered one of the hallmark during tumour development (Munkley J et al. 2016).

A second problem in studying glycans is because the final structures cannot be predicted simply by analysing expression of the relevant enzymes involved in the biosynthetic process. Glycoconjugate biosynthesis is influenced by several factors: i) activity of the metabolic pathways that provide the nucleotide-sugar substrates and their availability either in the cytosol and in the ER/Golgi lumen, which is conditioned by activity the specific transporters; ii) expression of the different glycosyltransferases, which add the monosaccharide units to the nascent oligosaccharide chain, or the glycosydases, which remodel the glycans; iii) localization of the enzymes in the secretory pathway and functionality and trafficking of the

Golgi cisternae and vesicles. Any modification in each of this factor can have profound effects on the final glycan composition (Varki A et al. 2009).

A third problem is methodological and it is due to the difficulties to analyse carbohydrates, in particular in very small amounts. In a complex glycoconjugate each monosaccharide can be bound to another monosaccaride in four different C positions, with either α or β configuration of the linkage. In the past, very large amounts of starting material were required to determine the structure of complex carbohydrates, in particular to allow purification of glycans from other macromolecules (nucleic acid, lipids and proteins), in order to analyse them by chemical methods. Even today, linkage analysis can be done only using GC-MS of PMAA (partially methylated alditol acetates) or, to completely resolve the structure, by NMR (Mulloy B et al. 2009). However, both methods require large amounts of pure glycan species. Alternatives have been developed, for instance using HPLC after derivatization of the released glycans using fluorescent probes. These latter techniques proved to be useful to separate the different oligosaccharide structures, but they are time consuming and require the availability of standard glycans; in any case, large amounts of starting sample material are needed. Another method relies on the use of exo- and endo-glycosydases to specifically remove monosaccharide residues (i.e. sialidases or galactosidases) or complete glycan structures (i.e. PNGase, or endoH glycosidase) (Mulloy B et al. 2009).

For the reasons stated above, the glycomic analyses are more complicated if compared to transcriptomic and proteomic analyses and despite the increasingly and widely recognized role of glycans in cell and tissue physiopathology, the number of studies is still limited.

Most of drawbacks of glycan analysis have been partially solved by the introduction of mass spectrometry technique in glycan studies, both ESI-MS and MALDI-TOF (Han L et al. 2013). Both techniques present advantages and disadvantages, but they can provide the glycoprofiles of the

cell or tissue under analysis, allowing easy comparison between different situations, i.e. health vs. disease or early vs. late developmental stages. Due to the high sensitivity of mass spectrometry, the amount of starting material required is usually lower compared to other methods. However, even if mass spectrometry is very precise to determine the composition of each glycan specie, a major drawback is that it is not possible to analyse the type of linkages (i.e. α or β and the C atom involved, if 1,2, 1,3, 1,4 or 1,6 bonds), thus impeding the conclusive identification of isomeric forms.

A second problem derives from the high sensitivity of the MS methods, in particular of MALDI-TOF, which makes the possible contamination from exogenous molecules a major problem. Since the sample needs to be extensively handled and many steps are required before MS analysis, it is possible to accumulate contaminants during the glycan purification and derivatization procedures. In particular, polyethylenglycole (PEG) and keratin represent the most frequently encountered challenge. PEG is usually contained in soaps and detergents and it can easily contaminate the sample. Keratin can be released by the skin during sample manipulation. To avoid contamination, it is better to work on a dedicated workbench in a cleaned room and with all the solutions prepared fresh daily. Another important consideration is to work with nitrile gloves, because latex may contain traces of natural rubber proteins.

In the last few years, MALDI-MS and MS/MS technique has quickly become a standard in glycomic analysis. Several databases for glycan profiles from human and mouse tissues are already available (Lisacek F et al. 2017). Glycoprofiles of mouse tissues have been obtained for normal mice and after knock-out of specific enzymes involved in glycan formation (North SJ et al. 2010). These results allowed correlating glycan structures with the phenotypic manifestations of the genetic ablation. Moreover, studies were also performed on patients affected by CDG diseases, further expanding our knowledge on glycan function (Yoshinao et al. 2006).

In spite of the increasing amount of glycoprofiles for tissues of animal experimental models, in particular mouse and rat, little information are currently available for glycans derived for mouse and rat PNS myelin. Previous data relied on results obtained using antibodies and enzymatic treatments (Sato Y 1999).

Very recently, the profile of mouse PNS myelin was obtained by bidimensional HPLC analysis (Yoshimura et al. 2017.). However, in this case, large amounts of myelin sample are needed. This can represent a limitation when working with very young animals, for instance to identify glycoconjugate changes during nerve development, or when studying models for demyelinating diseases, such as CMT knock-in mice.

The need to have a reliable method to obtain glycoprofiles of PNS myelin using very low amounts of starting material prompted us to start this study, aimed to set up a protocol to use MALDI-MS analysis. To this purpose, the published protocols already set up for other types of mouse tissue were modified, in order to be applied to myelin sample. The modified protocol that was set up in this study allowed to obtain reliable results and proved that it is possible to use very low amounts of starting material. However, it also evidenced the problems raised by exogenous contamination when using such low amounts of material and the absolute need to prevent it by working in highly controlled conditions.

The advantage of this procedure over the chromatographic method used by Yoshimura et al. is that, once the method is set, it is very fast and a complete analysis can be achieved in only two weeks treating up to 5 samples or more in parallel. The only step that requires a lot of time is to resolve the first glycoprofile by MS/MS analysis. Once the glycoprofile is obtained it can be used as reference to the fragmentation spectra obtained by subsequent analyses, thus avoiding the need to interpret each peak again.

Thus, this modified protocol will represent a valuable to analyse the glycan profile in mouse and rat models of human neurodegenerative or

other types of PNS diseases. Many CMT mouse models have been established (Bouhy et al. 2013), mimicking the mutations responsible for human diseases. This optimised protocol opens the way for difficult analysis, as in the case of these CMT mice models, in which the myelin is compromised and the quantity that can be recovered from the animal is low.

Few models for CMT1B and CMT1A diseases have been already identified and are made available by our collaborators at San Raffaele Hospital in Milano, to analyse changes of myelin glycosylation during the course of the experimental diseases. For instance, P0S63del mimics one of the most common mutations that affect MPZ in CMT1B patients (Blanquet-Grossard, F et al. 1995). PMP22Tr-J also recapitulates the findings in patients affected by CMT1A (Henry EW et al. 1983). In both conditions, the presence of the mutated or over expressed proteins induces ER stress and UPR (Brennan KM et al. 2015). It has been shown that ER-stress can also affect glycosylation patterns, thus it will be interesting to analyse the effect of these mutations on glycan expression. Another group of gain-of-function mutations recently identified in MPZ has a consequence the insertion of new glycosylation sites, such as the P0D61N mutant, thus increasing the number of sugar chains on the protein (Prada V et al. 2012). A mouse model for this mutation is currently under development by Prof. Grandis at the DINOGMI, University of Genova and Prof. D'Antonio at San Raffaele Hospital.

Other experimental models that would be worth to analyze are the mouse knock-out models for CDG, which mimic the mutations found in patients. Correlation between the histopathological finding in PNS nerves and glycans composition would provide useful information about the role of specific structures (i.e hybrid N-linked glycans) in myelin function.

The optimized protocol can be also applied to rat myelin. Rat models can also used to study diabetic neuropathy or nerve regeneration after nerve crushing or resection and to follow glycosylation change during foetal and

neonatal nerve myelinization or during aging. The small amount of tissue required also open the possibility to apply this technique also to the small human sural nerve biopsies, to analyze glycosylation changes during pathologies, which have been not performed yet, for ethical reasons.

Besides, MALDI ionization allows the use of a very low amount of sample. In this study it was possible to obtain good results using only 1 µl of the sample resuspended in 10 µl methanol, so it is possible to dry the remaining methanol under a gentle nitrogen stream and to save the permethylated sample for months, for instance to compare different pathogenic models in the same MALDI analysis.

The glycoprofile obtained in this study is in agreement with the very recent data obtained using bidimensional DEAE-HPLC analysis (Yoshimura et al. 2017). Most of the N-linked glycans are biantennary hybrid type, showing different degree of sulfatation. The HNK-1 epitope is not present, in contrast with previous findings, which indicated its presence on the motor fibers only (Löw K. et al. 1994), while core fucosylation is common. The presence of large amounts of hybrid N-linked glycans is puzzling, since this type of structure is uncommon on mature structures exposed on cell surface. Indeed, hybrid N-linked glycans are formed as biosynthetic intermediates in the ER/Golgi and they are mostly converted to complex ones. Terminal α3 and α6 mannose residues are not normally found on mature glycoproteins in vertebrates. Knock-out mice for mannosidase II, which allows the conversion of the hybrid structures to the complex ones by removing the α3 and α6 mannose residues, display large amounts of hybrid glycans on cell surfaces. These mice develop severe autoimmune responses resembling systemic lupus erythematosus (Green et al. 2007, Chui D et al. 2001). This finding has been related to the recognition of exposed mannose residue by the mannose binding lectins of the innate immune response, thus promoting complement activation and deposition (Ohta M et al. 1994). It is possible that the presence of hybrid

structures has some role in the compaction of the myelin sheaths and further studies are needed to solve this issue. Moreover, myelin damage caused by CMT mutations could cause exposure of these hybrid structures, causing complement activation. Thus, it would important to verify if they have a possible involvement in accelerating of de-myelination process.

Another interesting feature of the myelin N-linked structure is the significant presence of sulfated structures. The presence of sulfate is essential for myelin function. Indeed, knock-out mice for GlcNAc6ST-1 sulfotransferase show loss of myelin compaction and axonal degeneration (Yoshimura et al. 2017). The important role of negative charges in myelin N-linked glycans is also highlighted by the presence of sialic acid. In other species, including humans, the presence of negative charges is also ensured by the HNK-1 epitope, which is characterized by the presence of both glucuronic acid and sulfate (Löw K. et al. 1994). It is interesting to note that the HNK-1 is the antigen recognized by auto-antibodies in acquired human neuropathies, highlighting also the importance of glycans to promote immune activation against myelin in some types of human neurodegenerative diseases (Burger D et al. 1992).

O-linked glycans were not found in our analysis. This is consistent with previous data, which did not report their presence in large amounts, at least in compact myelin. However, it is not possible to exclude that they could be present in very low amounts. Moreover, analysis of O-linked glycans is more technically challenging. The first one is that glycan release need to be done using a chemical method and not an enzymatic one. PNGase, which is used to release N-linked glycan from the Asn, is a very active enzyme that works well in most experimental conditions, even in the presence of moderate detergent concentrations or high salts. On the other hand, O-glycosidases, which release the glycans from the Ser o Thr residues, are available, but have a very restrictive specificity and their activity is quite low. For this reason, a chemical method, β-elimination in the alkaline

conditions in the presence of reducing agents is the preferred method (North SJ et al. 2010). However, this procedure can lead to damage of the glycan structure, the so-called “peeling” reaction, thus affecting glycan recovery. For this reason, analysis of O-linked glycans should be performed using very large amounts of starting material.

Finally, this procedure could be also applied to the analysis of glycolipids. Indeed, after myelin purification, the following step is represented by a modified Folch extraction. With this method, all the phospholipids and sphingolipids are supposed to be extracted in the organic phase. Analysis of the lipid fraction was beyond the scope of this study. However, it is important to keep in mind that glycolipids can have also profound effects on myelin function.

In conclusion, the methods optimised in our laboratories have been demonstrated to be highly sensitive and reproducible and, together with our data, may be a starting point to understand the importance of myelin in the glycosylation of the PNS.

References

Arthur-Farraj PJ, Latouche M, Wilton DK, Quintes S, Chabrol E, Banerjee A, Woodhoo A, Jenkins B, Rahman M, Turmaine M, Wicher GK, Mitter R, Greensmith L, Behrens A, Raivich G, Mirsky R, Jessen KR (2012) c-Jun reprograms Schwann cells of injured nerves to generate a repair cell essential for regeneration. Neuron. 75: 633-47.

Bird TD. Charcot-Marie-Tooth Neuropathy Type 2. (1998) Sep 24 [Updated 2016 Apr 14]. In: Adam MP, Ardinger HH, Pagon RA, et al., editors. GeneReviews®. Seattle (WA): University of Washington, Seattle.

Blanquet-Grossard F, Pham-Dinh, D, Dautigny A, Latour, P, Bonnebouche C, Corbillon E, Chazot G. and Vandenberghe A. (1995), Charcot-Marie-Tooth type 1B neuropathy: third mutation of serine 63 codon in the major peripheral myelin glycoprotein P0 gene. Clinical Genetics, 48: 281–283

Bouhy D, Timmerman V. (2013) Animal models and therapeutic prospects for Charcot-Marie-Tooth disease. Ann Neurol. Sep; 74(3):391-6

Brennan KM, Bai Y, Shy ME (2015) Demyelinating CMT- what's known, what's new and what's in store? Neurosci Lett. Jun 2; 596:14-26.

Brunden KR. (1992) Age-dependent changes in the oligosaccharide structure of the major myelin glycoprotein, P0. J Neurochem. 58: 1659-66.

Burger D, Perruisseau G., Simon M. and Steck A.K. (1992) Comparison of the N-linked oligosaccharide structures of the two major human myelin glycoproteins MAG and P0: assessment of the structures bearing the epitope for HNK-1 and human monoclonal immunoglobulin M found in demyelinating neuropathy. J. Neurochem, 58:854–861

Burger D, Simon M, Perruisseau G, Steck AJ (1990) The epitope(s) recognized by HNK-1 antibody and IgM paraprotein in neuropathy is present on several N-linked oligosaccharide structures on human P0 and myelin-associated glycoprotein. J Neurochem.54:1569-75.

Hellerqvist CG (1990) Linkage Analysis Using Lindberg Method Methods in Enzymology Vol.193, 30

Ceroni A, Maass K., Geyer H, Geyer R, Dell A, and Haslam SM (2008) GlycoWorkbench. A tool for the computer-assisted annotation of mass spectra of glycans. J Proteome Res. Apr; 7(4):1650-9.

Chui D, Sellakumar G, Green RS, Sutton-Smith M, McQuistan T, Marek KW, Morris HR, Dell A, and Marth JD (2001) Genetic remodeling of protein glycosylation in vivo induces autoimmune disease PNAS 98 (3) 1142-1147

Damerell D, Ceroni A, Maass K, Ranzinger R, Dell A, Haslam SM. (2015) Annotation of glycomics MS and MS/MS spectra using the GlycoWorkbench software tool. Methods Mol Biol. 1273:3-15.

Dewal MB, DiChiara AS, Antonopoulos A, Taylor RJ, Harmon CJ, Haslam SM, Dell A, Shoulders MD. (2015) XBP1s Links the Unfolded Protein Response to the Molecular Architecture of Mature N-Glycans. Chem Biol. 22:1301-12.

D'Urso D, Brophy PJ, Staugaitis SM, Gillespie CS, Frey AB, Stempak JG, Colman DR (1990) Protein zero of peripheral nerve myelin: Biosynthesis, membrane insertion, and evidence for homotypic interaction Cell Neuron Volume 4, Issue 3, p449–460, March

Eichberg J. (2002) Myelin P0: new knowledge and new roles. Neurochem Res. 27:1331-40.

Eichberg, J. & Iyer, S. (1996) Phosphorylation of myelin proteins: Recent advances Neurochem Res 21: 527

Emery B (2013) Playing the Field: Sox10 Recruits Different Partners to Drive Central and Peripheral Myelination. PLoS Genetic, 10.

Fasano A, Amoresano A, Rossano R, Carlone G, Carpentieri A, Liuzzi GM, Pucci P, Riccio P (2008) The different forms of PNS myelin P0 protein within and outside lipid rafts. J Neurochem. 107:291-301.

Field MC, Wing DR, Dwek RA, Rademacher TW, Schmitz B, Bollensen E, Schachner M (1992) Detection of multisulfated N-linked glycans in the L2/HNK-1 carbohydrate epitope expressing neural adhesion molecule P0. J Neurochem.58:993-1000.

Filbin MT and Tennekoon GI (1991) The role of complex carbohydrates in adhesion of the myelin protein, P0. Neuron. 7:845-55.

Freeze HH, Schachter H, Kinoshita T. (2017) Genetic Disorders of Glycosylation. In: Varki A, Cummings RD, Esko JD, et al., editors. Essentials of Glycobiology [Internet]. 3rd edition. Cold Spring Harbor (NY): Cold Spring Harbor Laboratory Press; 2015-2017. Chapter 45.

Gallego RG, Blanco JL, Thijssen-van Zuylen CW, Gotfredsen CH, Voshol H, Duus JØ, Schachner M, Vliegenthart JF. (2001) Epitope diversity of N-glycans from bovine peripheral myelin glycoprotein P0 revealed by mass spectrometry and nano probe magic angle spinning 1H NMR spectroscopy. J Biol Chem. 276:30834-44.

Grandis M, Vigo T, Passalacqua M, Jain M, Scazzola S, La Padula V, Brucal M, Benvenuto F, Nobbio L, Cadoni A, Mancardi GL, Kamholz J, Shy ME, Schenone A (2008) Different cellular and molecular mechanisms for early and late-onset myelin protein zero mutations. Hum Mol Genet. 17:1877-89

Green RS, Stone EL, Tenno M, Lehtonen E, Farquhar MG., Marth JD (2007) Mammalian N-Glycan Branching Protects against Innate Immune

Self-Recognition and Inflammation in Autoimmune Disease Pathogenesis Immunity, Volume 27, Issue 2, 308-320

Han L, Costello CE (2013) Mass Spectrometry of Glycans. Biochemistry 78(7):710-720.

Henry EW, et al., Comparison of Trembler and Trembler-J mouse phenotypes: varying severity of peripheral hypomyelination (1983) J Neuropathol Exp Neurol. Nov;42 (6):688-706

Jang-Lee, J., North, S. J., Sutton-Smith, M., Goldberg, D., Panico, M., Morris, H., Haslam, S., and Dell, A. (2006) Glycomic profiling of cells and tissues by mass spectrometry: fingerprinting and sequencing methodologies. Methods in Enzymology 415, 59-86

Khoo K-H, Yu S-I, (2010) Chapter One-Mass Spectrometric Analysis of Sulfated N- and O-Glycans Editor(s): Minoru Fukuda, In Methods in Enzymology, Academic Press, Volume 478, Pages 3-26

Kirschner, DA and Blaurock, AE Organization, phylogenetic variations and dynamic transitions of myelin (1992) In R. E. Martenson (ed.), Myelin: biology and chemistry. Boca Raton, pp 3-78

Kirschner, DA, Wrabetz L and Feltri ML (2004) Chapter 20 - The P0 Gene, In Myelin Biology and Disorders, Academic Press, San Diego, Pages 523-545

Kizuka Y, Kitazume S, Taniguchi N (2017) N-glycan and Alzheimer's disease. Biochim Biophys Acta. pii: S0304-4165(17)30137-X.

Krasnewich D, O'Brien K and Spark S (2007) Clinical Features in Adults with Congenital Disorders of Glycosylation Type Ia (CDG-Ia) Am. J. Med. Genetics Part C 145C:302–306

Larsen RD, Rivera-Marrerot CA, Ernst LK, Cummings RD, Q, and Lowe JB (1990) Frameshift and Nonsense Mutations in a Human Genomic

Sequence Homologous to a Murine UDP-Gal&D-Gal(1,4)-D-GlcNAc CY(1,3)- Galactosyltransferase cDNA JBC Vol. 265, No. 12, Issue of April 25, pp. 7055-7061

Lisacek F, Mariethoz J, Alocci D, Rudd PM, Abrahams JL, Campbell MP, Packer NH, Ståhle J, Widmalm G, Mullen E, Adamczyk B, Rojas-Macias MA, Jin C, Karlsson NG (2017) Databases and Associated Tools for Glycomics and Glycoproteomics. In: Lauc G., Wuhrer M (eds) High-Throughput Glycomics and Glycoproteomics. Methods in Molecular Biology, vol 1503. Humana Press, New York, NY

Löw K, Orberger G, Schmitz B, Martini R, Schachner M. (1994) The L2/HNK-1 carbohydrate is carried by the myelin associated glycoprotein and sulfated glucuronyl glycolipids in muscle but not cutaneous nerves of adult mice. Eur J Neurosci. 6:1773-81

Martini R (1997) Animal models for inherited peripheral neuropathies. J Anat 191:321–336.

Martini R, Bollensen E, Schachner M. (1998) Immunocytological localization of the major peripheral nervous system glycoprotein P0 and the L2/HNK-1 and L3 carbohydrate structures in developing and adult mouse sciatic nerve. Dev Biol. 129:330-8.

Morelle W, Michalski JC (2007) Analysis of protein glycosylation by mass spectrometry Nature Protocols 2, 2007, - 1585-1602

Mulloy B, Hart GW, Stanley P. (2009) Structural Analysis of Glycans. In: Varki A, Cummings RD, Esko JD, et al., editors. Essentials of Glycobiology. 2nd edition. Cold Spring Harbor (NY): Cold Spring Harbor Laboratory Press; Chapter 47. Available from: https://www.ncbi.nlm.nih.gov/books/NBK1898/

Munkley J, Elliott DJ. (2016) Hallmarks of glycosylation in cancer Oncotarget 7(23):35478-35489.

North SJ, Jang-Lee J, Harrison R, Canis K, Ismail MN, Trollope A, Antonopoulos A, Pang PC, Grassi P, Al-Chalabi S, Etienne AT, Dell A, Haslam SM (2010) Chapter Two - Mass Spectrometric Analysis of Mutant Mice, Editor(s): Minoru Fukuda, In Methods in Enzymology, Academic Press, Volume 478, Pages 27-77

Norton WT, Poduslo SE (1973) Myelination in rat brain: method of myelin isolation. J Neurochem 4: 749-57

Ohta M, Kawasaki T. (1994) Complement-dependent cytotoxic activity of serum mannan-binding protein towards mammalian cells with surface-exposed high-mannose type glycans. Glycoconj J. Aug; 11(4):304-8.

Pareyson D, Saveri P, Pisciotta C. (2017) New developments in Charcot-Marie-Tooth neuropathy and related diseases. Curr Opin Neurol. Jul 3.

Pascual-Castroviejo I1, Pascual-Pascual SI, Quijano-Roy S, Gutiérrez-Molina M, Morales MC, Velázquez-Fragua R, Maties M. (2006) Cerebellar ataxia of Norman-Jaeken. Presentation of seven Spanish patients. Rev Neurol. Jun 16-30; 42(12):723-8.

Patzig J, Jahn O, Tenzer S, Wichert SP, de Monasterio-Schrader P, Rosfa S, Kuharev J, Yan K, Bormuth I, Bremer J, Aguzzi A, Orfaniotou F, Hesse D, Schwab MH, Möbius W, Nave KA, Werner HB. (2011) Quantitative and integrative proteome analysis of peripheral nerve myelin identifies novel myelin proteins and candidate neuropathy loci. J Neurosci. 31:16369-86.

Poduslo JF (1985) Posttranslational protein modification: biosynthetic control mechanisms in the glycosylation of the major myelin glycoprotein by Schwann cells. J Neurochem. 44:1194-206.

Prada V, Callegari I, Salerno A, Passalacqua M, Tonetti M, Schenone A, Grandis M. (2015) Therapeutic options for MPZ mutation causing misglycosylation. J. Peripher Nerv Syst (Supplement): S1–S31.

Prada V, Passalacqua M, Bono M, Luzzi P, Scazzola S, Nobbio LA, Capponi S, Bellone E, Mandich P, Mancardi G, Shy M, Schenone A, Grandis M. (2012) Gain of glycosylation: a new pathomechanism of myelin protein zero mutations. Ann Neurol. 71:427-31.

Pronker MF, Lemstra S, Snijder J, Heck AJ, Thies-Weesie DM, Pasterkamp RJ, Janssen BJ. (2016) Structural basis of myelin-associated glycoprotein adhesion and signalling. Nat Commun. Dec 6; 7:13584.

Pusch W, Flocco MT, Leung SM, Thiele H, Kostrzewa M (2003) Mass spectrometry-based clinical proteomics. Pharmacogenomics. Jul; 4(4):463-76.

Quarles RH and Morell P (2006) Chapter 4: Myelin Formation, Structure and Biochemistry of Basic Neurochemistry: Molecular, Cellular and Medical Aspects. 6th edition. Pages 69-94

Raine, C. S. In Myelin, 2nd ed.; P. Morell; New York: Plenum, 1984; 1–41

Rotenstein L, Herath K, Gould RM, de Bellard ME. (2008) Characterization of the shark myelin P0 protein. Brain Behav Evol. 72:48-58.

Ruiz-Matute AI, Hernández-Hernández O, Rodríguez-Sánchez S, Sanz ML, Martínez-Castro I (2011) Derivatization of carbohydrates for GC and GC–MS analyses, In Journal of Chromatography B, Volume 879, Issues 17–18, Pages 1226-1240

Sato Y and Endo T. (2000) Alterations with age of the neurons expressing P (0) in the rat spinal cord. Neurosci Lett. 281:41-4.

Sato Y, Kimura M, Yasuda C, Nakano Y, Tomita M, Kobata A, Endo T (1999) Evidence for the presence of major peripheral myelin glycoprotein P0 in mammalian spinal cord and a change of its glycosylation state during aging. Glycobiology. 9:655-60.

Scherer SS, Wrabetz L. (2008) Molecular mechanisms of inherited demyelinating neuropathies. Glia. 56:1578-89.

Scott H and Panin VM -N-glycosylation in Regulation of the Nervous System (2014) Adv Neurobiol. 9: 367–394.

Sedzik J, Jastrzebski JP, Grandis M (2015) Glycans of myelin proteins. J Neurosci Res. Jan; 93(1):1-18

Shapiro L, Doyle JP, Hensley P, Colman DR, Hendrickson WA. (1996) Crystal Structure of the Extracellular Domain from P0, the Major Structural Protein of Peripheral Nerve Myelin Neuron, Volume 17, Issue 3, 435-449

Shy ME, Jáni A, Krajewski K, Grandis M, Lewis RA, Li J, Shy RR, Balsamo J, Lilien J, Garbern JY, Kamholz J (2004) Phenotypic clustering in MPZ mutations. Brain 127(Pt 2):371-84·March

Small, J. R., Ghabriel, M. N., & Allt, G. (1987). The development of Schmidt-Lanterman incisures: an electron microscope study. Journal of Anatomy, 150, 277–286.
Spiegel I & Peles E (2002) Cellular junctions of myelinated nerves (Review) Molecular Membrane Biology Vol. 19, 2

Stanley P, Schachter H, Taniguchi N (2009) N-Glycans. In: Varki A, Cummings RD, Esko JD, et al., editors. Essentials of Glycobiology. 2nd edition. Cold Spring Harbor (NY): Cold Spring Harbor Laboratory Press; Chapter 8. Available from: https://www.ncbi.nlm.nih.gov/books/NBK1917/

Varki A, Kannagi R, Toole BP (2009) Glycosylation Changes in Cancer. In: Varki A, Cummings RD, Esko JD, et al., editors. Essentials of Glycobiology. 2nd edition. Cold Spring Harbor (NY): Cold Spring Harbor Laboratory Press; Chapter 44. Available from: https://www.ncbi.nlm.nih.gov/books/NBK1963/

Varki A. (2010) Uniquely human evolution of sialic acid genetics and biology. Proceedings of the National Academy of Sciences of the United States of America. 107:8939-8946.

Vogt G, Chapgier A, Yang K, Chuzhanova N, Feinberg J, Fieschi C, Boisson-Dupuis S, Alcais A, Filipe-Santos O, Bustamante J, de Beaucoudrey L, Al-Mohsen I, Al-Hajjar S, Al-Ghonaium A, Adimi P, Mirsaeidi M, Khalilzadeh S, Rosenzweig S, de la Calle Martin O, Bauer TR, Puck JM, Ochs HD, Furthner D, Engelhorn C, Belohradsky B, Mansouri D, Holland SM, Schreiber RD, Abel L, Cooper DN, Soudais C, Casanova JL. (2005) Gains of glycosylation comprise an unexpectedly large group of pathogenic mutations. Nat Genet. 37:692-700.

Vogt G, Vogt B, Chuzhanova N, Julenius K, Cooper DN, Casanova JL (2007) Gain-of-glycosylation mutations. Curr Opin Genet Dev. 17:245-51.

Voshol H.,Van Zuylen C. W.,Orberger G.,Vliegenthart J. F.and Schachner M (1996) Structure of the HNK-1 carbohydrate epitope on bovine peripheral myelin glycoprotein P0. J. Biol. Chem. 271, 22957–22960.

Wessel, D. and Flügge, U.I (1984) A method for the quantitative recovery of protein in dilute solution in the presence of detergents and lipids Anal. Biochem. 138 141–143.

Xie B, Luo X, Zhao C, Priest CM, Chan SY, O' Connor PB, Kirschner DA, Costello CE. (2007) Molecular Characterization of Myelin Protein Zero in Xenopus laevis Peripheral Nerve: Equilibrium between Non-Covalently Associated Dimer and Monomer. Int J Mass Spectrom. 268:304-315.

Ye Z, Marth JD (2004) N-glycan branching requirement in neuronal and postnatal viability Glycobiology, Volume 14, Issue 6, 1 June Pages 547–558.

Yoshimura T, Hayashi A, Handa-Narumi M, Yagi H, Ohno N, Koike T, Yamaguchi Y, Uchimura K, Kadomatsu K, Sedzik J, Kitamura K, Kato K, Trapp BD, Baba H, Ikenaka K (2017) GlcNAc6ST-1 regulates sulfation of N-glycans and myelination in the peripheral nervous system. Sci Rep. 7:42257.

Yoshinao W (2006) Mass spectrometry for congenital disorders of glycosylation, CDG, In Journal of Chromatography B, Volume 838, Issue 1, Pages 3-8

Zaia J (2010) Mass Spectrometry and Glycomics OMICS. Aug; 14(4): 401–418.

Supplemental tables and figures

Protein	Peptide	Label	Start	End
Myelin Protein P0	YQPEGGR	1:T003	68	74
Myelin Protein P0	YQPEGGR	1:T003	68	74
Myelin Protein P0	YQPEGGR	1:T003	68	74
Myelin Protein P0	YQPEGGR	1:T003	68	74
Myelin Protein P0	YQPEGGR	1:T003	68	74
Myelin Protein P0	YQPEGGR	1:T003	68	74
Myelin Protein P0	YQPEGGR	1:T003	68	74
Myelin Protein P0	YQPEGGRDAISIFHYAK	1:T003-004	68	84
Myelin Protein P0	YQPEGGRDAISIFHYAKGQPYI-DEVGAFKERIQWVGDPR	1:T003-007	68	106
Myelin Protein P0	DAISIFHYAKGQPYIDEVGAFK-ERIQWVGDPRWK	1:T004-008	75	108
Myelin Protein P0	GQPYIDEVGAFK	1:T005	85	96
Myelin Protein P0	GQPYIDEVGAFK	1:T005	85	96
Myelin Protein P0	GQPYIDEVGAFK	1:T005	85	96
Myelin Protein P0	GQPYIDEVGAFKER	1:T005-006	85	98
Myelin Protein P0	GQPYIDEVGAFK	1:T005	85	96
Myelin Protein P0	GQPYIDEVGAFK	1:T005	85	96
Myelin Protein P0	GQPYIDEVGAFKER	1:T005-006	85	98
Myelin Protein P0	GQPYIDEVGAFK	1:T005	85	96
Myelin Protein P0	GQPYIDEVGAFK	1:T005	85	96
Myelin Protein P0	GQPYIDEVGAFK	1:T005	85	96
Myelin Protein P0	GQPYIDEVGAFK	1:T005	85	96
Myelin Protein P0	GQPYIDEVGAFK	1:T005	85	96
Myelin Protein P0	GQPYIDEVGAFK	1:T005	85	96
Myelin Protein P0	GQPYIDEVGAFK	1:T005	85	96
Myelin Protein P0	GQPYIDEVGAFK	1:T005	85	96
Myelin Protein P0	GQPYIDEVGAFK	1:T005	85	96
Myelin Protein P0	GQPYIDEVGAFK	1:T005	85	96
Myelin Protein P0	GQPYIDEVGAFK	1:T005	85	96
Myelin Protein P0	GQPYIDEVGAFK	1:T005	85	96
Myelin Protein P0	ERIQWVGDPR	1:T006-007	97	106
Myelin Protein P0	ERIQWVGDPR	1:T006-007	97	106
Myelin Protein P0	IQWVGDPR	1:T007	99	106
Myelin Protein P0	IQWVGDPR	1:T007	99	106
Myelin Protein P0	IQWVGDPRWK	1:T007-008	99	108
Myelin Protein P0	IQWVGDPRWK	1:T007-008	99	108

Myelin Protein P0	IQWVGDPR	1:T007	99	106
Myelin Protein P0	IQWVGDPRWK	1:T007-008	99	108
Myelin Protein P0	IQWVGDPR	1:T007	99	106
Myelin Protein P0	IQWVGDPR	1:T007	99	106
Myelin Protein P0	IQWVGDPR	1:T007	99	106
Myelin Protein P0	IQWVGDPR	1:T007	99	106
Myelin Protein P0	IQWVGDPR	1:T007	99	106
Myelin Protein P0	IQWVGDPR	1:T007	99	106
Myelin Protein P0	IQWVGDPR	1:T007	99	106
Myelin Protein P0	DGSIVIHNLDYSDNGTFTCDVK	1:T009*	109	130
Myelin Protein P0	DGSIVIHNLDYSDNGTFTCDVK	1:T009*	109	130
Myelin Protein P0	NPPDIVGK	1:T010	131	138
Myelin Protein P0	NPPDIVGK	1:T010	131	138
Myelin Protein P0	NPPDIVGK	1:T010	131	138
Myelin Protein P0	TSQVTLYVFEK	1:T011	139	149
Myelin Protein P0	TSQVTLYVFEK	1:T011	139	149
Myelin Protein P0	TSQVTLYVFEK	1:T011	139	149
Myelin Protein P0	VPTR	1:T012	150	153
Myelin Protein P0	VPTRYGVVLGAVIGGILGVVLL-LLLLFYLIRYCWLRR	1:T012-015*	150	186
Myelin Protein P0	VPTRYGVVLGAVIGGILGVVLL-LLLLFYLIRYCWLRR	1:T012-015*	150	186
Myelin Protein P0	VPTR	1:T012	150	153
Myelin Protein P0	VPTR	1:T012	150	153
Myelin Protein P0	VPTR	1:T012	150	153
Myelin Protein P0	VPTR	1:T012	150	153
Myelin Protein P0	YGVVLGAVIGGILGVVLLLLLLF-YLIRYCWLR	1:T013-014*	154	185
Myelin Protein P0	YGVVLGAVIGGILGVVLLLLLLF-YLIRYCWLRRQAALQRR	1:T013-017*	154	193
Myelin Protein P0	YCWLR	1:T014*	181	185
Myelin Protein P0	YCWLRRQAALQR	1:T014-016*	181	192
Myelin Protein P0	YCWLRR	1:T014-015*	181	186
Myelin Protein P0	YCWLRRQAALQRR	1:T014-017*	181	193
Myelin Protein P0	YCWLR	1:T014*	181	185
Myelin Protein P0	YCWLRRQAALQR	1:T014-016*	181	192
Myelin Protein P0	YCWLR	1:T014*	181	185
Myelin Protein P0	YCWLRR	1:T014-015*	181	186
Myelin Protein P0	YCWLR	1:T014*	181	185
Myelin Protein P0	R	1:T015	186	186
Myelin Protein P0	RQAALQRRLSAMEK	1:T015-018	186	199
Myelin Protein P0	QAALQRR	1:T016-017	187	193
Myelin Protein P0	QAALQRR	1:T016-017	187	193
Myelin Protein P0	QAALQRR	1:T016-017	187	193

Myelin Protein P0	QAALQRR	1:T016-017	187	193
Myelin Protein P0	QAALQRR	1:T016-017	187	193
Myelin Protein P0	QAALQRR	1:T016-017	187	193
Myelin Protein P0	QAALQRR	1:T016-017	187	193
Myelin Protein P0	RLSAMEK	1:T017-018	193	199
Myelin Protein P0	RLSAMEK	1:T017-018	193	199
Myelin Protein P0	RLSAMEK	1:T017-018	193	199
Myelin Protein P0	RLSAMEK	1:T017-018	193	199
Myelin Protein P0	RLSAMEK	1:T017-018	193	199
Myelin Protein P0	RLSAMEKGRFHK	1:T017-020	193	204
Myelin Protein P0	RLSAMEKGR	1:T017-019	193	201
Myelin Protein P0	LSAMEK	1:T018	194	199
Myelin Protein P0	LSAMEKGRFHK	1:T018-020	194	204
Myelin Protein P0	LSAMEKGRFHK	1:T018-020	194	204
Myelin Protein P0	LSAMEKGRFHKSSK	1:T018-021	194	207
Myelin Protein P0	LSAMEKGR	1:T018-019	194	201
Myelin Protein P0	LSAMEKGRFHK	1:T018-020	194	204
Myelin Protein P0	FHK	1:T020	202	204
Myelin Protein P0	FHK	1:T020	202	204
Myelin Protein P0	FHKSSKDSSK	1:T020-022	202	211
Myelin Protein P0	FHKSSKDSSK	1:T020-022	202	211
Myelin Protein P0	FHKSSKDSSK	1:T020-022	202	211
Myelin Protein P0	FHKSSKDSSKR	1:T020-023	202	212
Myelin Protein P0	FHKSSKDSSKR	1:T020-023	202	212
Myelin Protein P0	FHK	1:T020	202	204
Myelin Protein P0	FHKSSKDSSKR	1:T020-023	202	212
Myelin Protein P0	FHKSSKDSSKRGR	1:T020-024	202	214
Myelin Protein P0	SSKDSSKR	1:T021-023	205	212
Myelin Protein P0	SSKDSSK	1:T021-022	205	211
Myelin Protein P0	SSKDSSKR	1:T021-023	205	212
Myelin Protein P0	SSKDSSKR	1:T021-023	205	212
Myelin Protein P0	SSKDSSKR	1:T021-023	205	212
Myelin Protein P0	SSKDSSKR	1:T021-023	205	212
Myelin Protein P0	SSKDSSKRGR	1:T021-024	205	214
Myelin Protein P0	DSSKRGR	1:T022-024	208	214
Myelin Protein P0	DSSKR	1:T022-023	208	212
Myelin Protein P0	DSSK	1:T022	208	211
Myelin Protein P0	DSSKRGR	1:T022-024	208	214
Myelin Protein P0	GRQTPVLYAMLDHSRSTK	1:T024-026	213	230
Myelin Protein P0	GRQTPVLYAMLDHSRSTK	1:T024-026	213	230
Myelin Protein P0	GRQTPVLYAMLDHSR	1:T024-025	213	227
Myelin Protein P0	STKAASEK	1:T026-027	228	235
Myelin Protein P0	STKAASEK	1:T026-027	228	235

Myelin Protein P0	STKAASEKK	1:T026-028	228	236
Myelin Protein P0	STKAASEK	1:T026-027	228	235
Myelin Protein P0	AASEKK	1:T027-028	231	236
Myelin Protein P0	AASEKK	1:T027-028	231	236
Myelin Protein P0	AASEKK	1:T027-028	231	236
Myelin Protein P0	AASEK	1:T027	231	235
Myelin Protein P0	AASEKKSK	1:T027-029	231	238
Myelin Protein P0	AASEKKSKGLGESR	1:T027-030	231	244
Myelin Protein P0	K	1:T028	236	236
Myelin Protein P0	GLGESR	1:T030	239	244
Myelin Protein P0	GLGESRK	1:T030-031	239	245
Myelin Protein P0	GLGESRK	1:T030-031	239	245
Myelin Protein P0	GLGESR	1:T030	239	244
Myelin Protein P0	GLGESRKDK	1:T030-032	239	247
Myelin Protein P0	GLGESRKDK	1:T030-032	239	247
Myelin Protein P0	GLGESRKDKK	1:T030-033	239	248

ST1. MPZ peptides found in the ESI analysis.

Accession	Entry	mW (Da)	pI (pH)	PLGS Score
TRYP_PIG	TRYP_PIG	24393	6,9141	10794,42
B2RSN3_MOUSE	B2RSN3_MOUSE	49920	4,5908	4638,735
MYP0_MOUSE	MYP0_MOUSE	27604	9,7515	3947,008
E9QQ57_MOUSE	E9QQ57_MOUSE	147536	8,5488	3938,486
PRAX_MOUSE	PRAX_MOUSE	147594	8,3584	3689,903
F6RT34_MOUSE	F6RT34_MOUSE	23182	11,2778	2220,164
F6TYB7_MOUSE	F6TYB7_MOUSE	21167	11,1343	2195,693
TBA1A_MOUSE	TBA1A_MOUSE	50103	4,7622	2008,445
TBA1B_MOUSE	TBA1B_MOUSE	50119	4,7622	1784,487
TBA4A_MOUSE	TBA4A_MOUSE	49892	4,752	1026,153
ALBU_MOUSE	ALBU_MOUSE	68647	5,6763	382,7863
CD9_MOUSE	CD9_MOUSE	25240	6,9639	326,9419
NDUF3_MOUSE	NDUF3_MOUSE	20720	8,0273	270,2818
AGK_MOUSE	AGK_MOUSE	46946	8,4419	211,6779
A0A140T8I6_MOUSE	A0A140T8I6_MOUSE	36076	10,4546	197,3638
AT1B1_MOUSE	AT1B1_MOUSE	35171	8,7817	197,2095

NFL_MOUSE	NFL_MOUSE	61471	4,415	195,2418
A2AHQ7_MOUSE	A2AHQ7_MOUSE	133722	5,937	172,1517
GLT10_MOUSE	GLT10_MOUSE	69071	8,417	170,4506
ISL2_MOUSE	ISL2_MOUSE	39702	8,0991	170,4261
CD69_MOUSE	CD69_MOUSE	22502	6,5859	170,1749
CN37_MOUSE	CN37_MOUSE	47093	9,2578	167,2831
G3UZY9_MOUSE	G3UZY9_MOUSE	14026	10,6875	161,5311
MSL1_MOUSE	MSL1_MOUSE	67277	9,2944	155,1338
A2AP78_MOUSE	A2AP78_MOUSE	18299	10,2085	154,8326
FA10_MOUSE	FA10_MOUSE	53983	5,3438	143,0321
Q6PCM4_MOUSE	Q6PCM4_MOUSE	66328	8,8652	142,8326
A0A0A6YWC8_MOUSE	A0A0A6YWC8_MOUSE	49162	4,8618	142,5211
A2ARR8_MOUSE	A2ARR8_MOUSE	39915	9,3896	140,6328
D3YYX3_MOUSE	D3YYX3_MOUSE	17386	8,8403	136,8201
Q99K53_MOUSE	Q99K53_MOUSE	79920	9,7163	133,8669
A0A0J9YU37_MOUSE	A0A0J9YU37_MOUSE	64611	6,1802	133,7945
GBA2_MOUSE	GBA2_MOUSE	103227	5,2192	133,1584
Q6NV92_MOUSE	Q6NV92_MOUSE	75901	9,6313	131,0092
Q7TMN8_MOUSE	Q7TMN8_MOUSE	66999	9,1743	128,6747
A2ARX1_MOUSE	A2ARX1_MOUSE	60276	9,3105	128,23
TLR8_MOUSE	TLR8_MOUSE	119282	6,9199	125,4914
D3Z5Z2_MOUSE	D3Z5Z2_MOUSE	57364	9,3486	123,9828
RAB6A_MOUSE	RAB6A_MOUSE	23574	5,2266	123,8001
ZFP28_MOUSE	ZFP28_MOUSE	93249	9,3472	123,3146
G3X964_MOUSE	G3X964_MOUSE	80229	7,6055	119,3493
Q8BUQ3_MOUSE	Q8BUQ3_MOUSE	97193	9,3164	119,2382
ALD2_MOUSE	ALD2_MOUSE	36097	5,9326	117,9798
ZFP26_MOUSE	ZFP26_MOUSE	97925	8,168	116,8602
Q8BIB6_MOUSE	Q8BIB6_MOUSE	61091	8,9136	116,5319
Q8BLK6_MOUSE	Q8BLK6_MOUSE	66514	8,4888	115,8054
A2AHM2_MOUSE	A2AHM2_MOUSE	34502	9,3457	115,3875
NFM_MOUSE	NFM_MOUSE	95858	4,5571	98,7081
FRMD8_MOUSE	FRMD8_MOUSE	51795	5,9854	89,1637
Q3U4X8_MOUSE	Q3U4X8_MOUSE	104028	6,709	67,0747
ZC3HD_MOUSE	ZC3HD_MOUSE	203633	9,7646	60,9883
H7BX26_MOUSE	H7BX26_MOUSE	173839	6,7544	42,2316
F8WGF2_MOUSE	F8WGF2_MOUSE	164210	6,8291	33,9826
D3YVU4_MOUSE	D3YVU4_MOUSE	144760	8,1372	33,4279

ST2. In this table, all the hits for the ESI/MS analysis are reported.

Molecular ions $[M + Na]^+$	Structure
1579.8	GlcNAc2-Man5
1783.9	GlcNAc2-Man6
1999.1	GlcNAc3-Man4-Gal-Fuc
2040.1	GlcNAc4-Man3-Gal-Fuc
2081.1	GlcNAc5-Man3-Fuc
2156.1	GlcNAc3-Man3-Gal-Fuc-Neu5Ac
2244.2	GlcNAc4-Man3-Gal2-Fuc
2285.2	GlcNAc5-Man3-Gal-Fuc
2360.3	GlcNAc3-Man4-Gal-Fuc-NeuAc
2390.3	GlcNAc3-Man4-Gal-Fuc-NeuGc
2448.3	GlcNAc4-Man3-Gal3-Fuc
2564.4	GlcNAc3-Man5-Gal-Fuc-NeuAc
2594.4	GlcNAc3-Man5-Gal-Fuc-NeuGl
2605.3	GlcNAc4-Man3-Gal2-Fuc-NeuAc
2646.4	GlcNAc5-Man3-Gal-NeuAc
2722.4	GlcNAc3-Man4-Gal-Fuc-NeuAc2
2809.5	GlcNAc4-Man3-Gal3-Fuc-NeuAc
2839.5	GlcNAc4-Man3-Gal3-Fuc-NeuGc
2966.6	GlcNAc4-Man3-Gal2-Fuc-NeuAc2
2996.6	GlcNAc4-Man3-Gal2-Fuc-NeuAc-NeuGc
3013.6	GlcNAc4-Man4-Gal3-Fuc-NeuAc
3054.6	GlcNAc5-Man3-Gal3-Fuc-NeuAc

Table ST3. Neutral permethylated N-glycans found in positive ion mode analysis.

Molecular ions $[M + (n+1)Na-nH]^+$ (n = number of sulfated group)	Structure
1986.0	GlcNAc3-Hex5-Fuc-S
2072.9	GlcNAc3-Man4-Gal-Fuc
2086.9	GlcNAc3-Man4-Gal-Fuc-S
2252,9	GlcNAc3-Man3-Gal-Fuc-NeuAc-S
2369.1	GlcNAc3-Man4-Gal-Fuc-NeuAc
2399,1	GlcNAc3-Man4-Gal-Fuc-NeuGc
2456.0	GlcNAc3-Man4-Gal-NeuAc-S
2486.1	GlcNAc3-Man4-Gal-Fuc-NeuGc-S
2498.1	GlcNAc4-Man3-Gal-NeuAC-(S)
2573.2	GlcNAc3-Man5-Gal-Fuc-NeuAc
2661.1	GlcNAc3-Man5-Gal-Fuc-NeuAc-S
2702.1	GlcNAc4-Man3-Gal2-Fuc-NeuAc-S
2818.3	GlcNAc3-Man4-Gal-Fuc-NeuAc2-S
3071.2	GlcNAc4-Man3-Gal2-Fuc-NeuAc2-S

Table ST4. Polar permethylated N-glycans found in positive ion mode analysis.

Molecular ions $[M-H]^-$	Structure
1823.9	GlcNAc3-Hex5-Fuc-S
2027.0	GlcNAc3-Man4-Gal-Fuc
2041.1	GlcNAc3-Man4-Gal-Fuc-S
2206,1	GlcNAc3-Man3-Gal-Fuc-NeuAc-S
2411.1	GlcNAc3-Man4-Gal-NeuAc-S
2440.1	GlcNAc3-Man4-Gal-Fuc-NeuGc-S
2615.2	GlcNAc3-Man5-Gal-Fuc-NeuAc-S
2655.3	GlcNAc4-Man3-Gal2-Fuc-NeuAc-S
3024.4	GlcNAc4-Man3-Gal2-Fuc-NeuAc2-S

Table ST5. Polar permethylated N-glycans found in negative ion mode analysis.

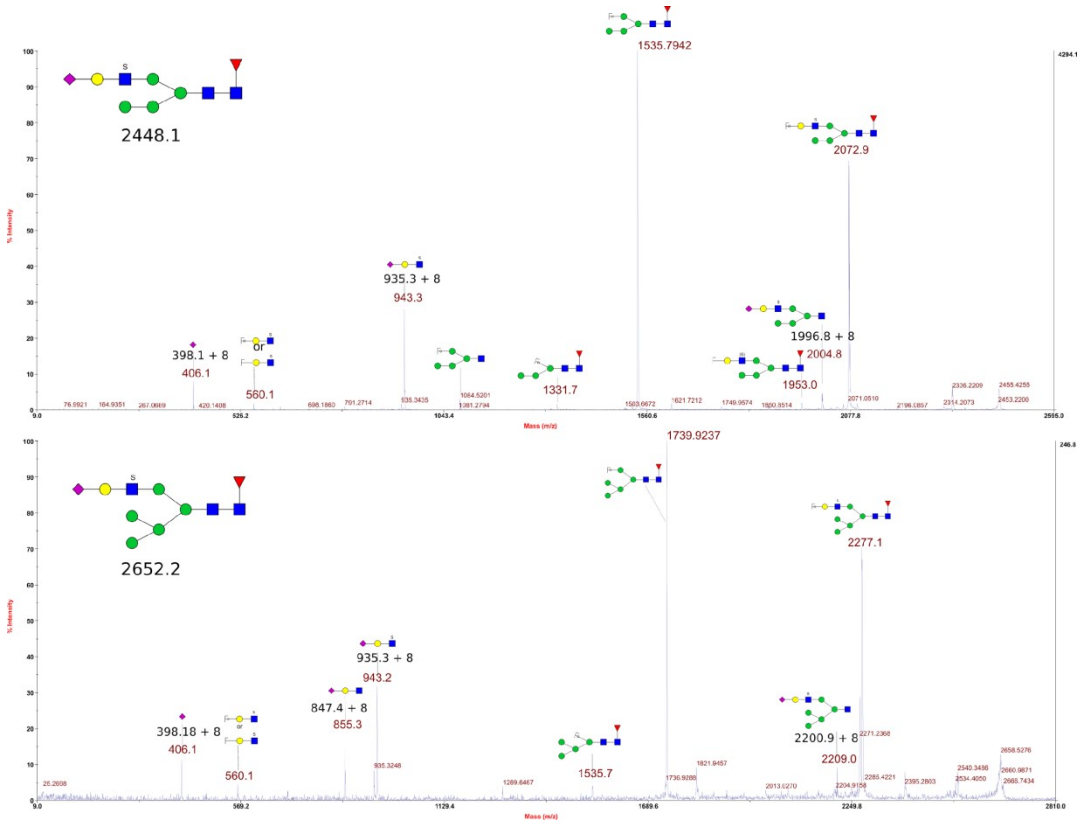

SF1. MS/MS spectra showing the modified weight of fragments caused by incomplete permethylation of the sialic acids.

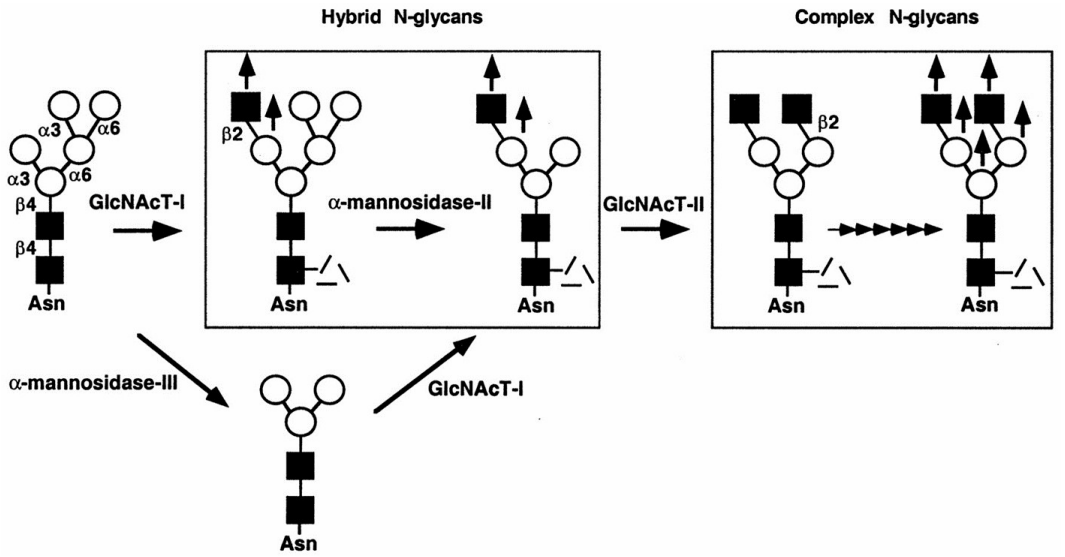

SF2. This image shows the metabolism of complex glycans from a high mannose. (Daniel Chui et al. 2001)